



Published in final edited form as:

Cell Rep. 2021 December 28; 37(13): 110178. doi:10.1016/j.celrep.2021.110178.

GM-CSF production by non-classical monocytes controls antagonistic LPS-driven functions in allergic inflammation

Kamaljeet Kaur¹, Holly Bachus², Crystal Lewis¹, Amber M. Papillion², Alexander F. Rosenberg¹, André Ballesteros-Tato², Beatriz León^{1,3,*}

¹Department of Microbiology, University of Alabama at Birmingham, Birmingham, AL 35294, USA

²Department of Medicine, Division of Clinical Immunology and Rheumatology, University of Alabama at Birmingham, Birmingham, AL 35294, USA

³Lead contact

SUMMARY

Lipopolysaccharide (LPS) can either promote or prevent T helper 2 (Th2) cell allergic responses. However, the underlying mechanism remains unknown. We show here that LPS activity switches from pro-pathogenic to protective depending on the production of granulocyte-macrophage colony-stimulating factor (GM-CSF) by non-classical monocytes. In the absence of GM-CSF, LPS can favor pathogenic Th2 cell responses by supporting the trafficking of lung-migratory dendritic cells (mDC2s) into the lung-draining lymph node. However, when non-classical monocytes produce GM-CSF, LPS and GM-CSF synergize to differentiate monocyte-derived DCs from classical Ly6C^{hi} monocytes that instruct mDC2s for Th2 cell suppression. Importantly, only allergens with cysteine protease activity trigger GM-CSF production by non-classical monocytes. Hence, the therapeutic effect of LPS is restricted to allergens with this enzymatic activity. Treatment with GM-CSF, however, restores the protective effects of LPS. Thus, GM-CSF produced by non-classical monocytes acts as a rheostat that fine-tunes the pathogenic and therapeutic functions of LPS.

Graphical Abstract

This is an open access article under the CC BY-NC-ND license (<http://creativecommons.org/licenses/by-nc-nd/4.0/>).

*Correspondence: bleon@uab.edu.

AUTHOR CONTRIBUTIONS

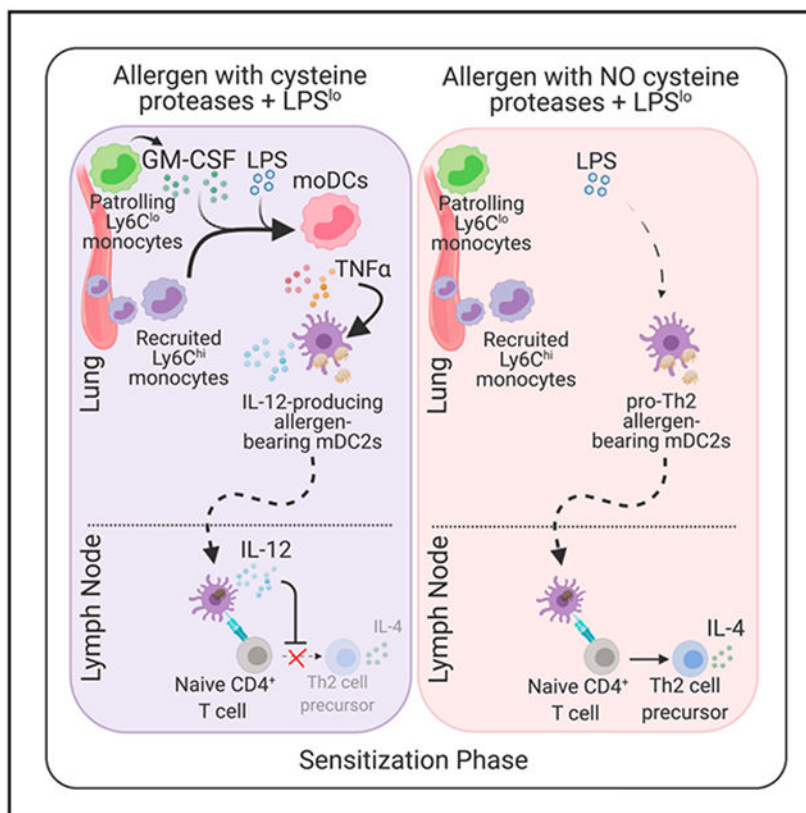
B.L. designed the study, performed experiments, and wrote the manuscript. K.K., H.B., B.L., C.L., and A.M.P. performed experiments. K.K. and B.L. analyzed the data. A.F.R. analyzed the RNA-seq data. A.B.-T. contributed to data interpretation and discussion. All authors reviewed the manuscript before submission.

SUPPLEMENTAL INFORMATION

Supplemental information can be found online at <https://doi.org/10.1016/j.celrep.2021.110178>.

DECLARATION OF INTERESTS

The authors declare no competing interests.



In brief

LPS can promote or prevent allergic sensitization. Kaur et al. demonstrate that GM-CSF segregates those different LPS-driven roles. Only allergens with cysteine protease activity trigger GM-CSF production by non-classical Ly6C^{lo} monocytes, preventing sensitization to LPS-containing allergens by modulating the function of classical Ly6C^{hi} monocytes and migratory dendritic cells.

INTRODUCTION

Allergic airway disease is the most common chronic disorder worldwide (Dharmage et al., 2019). Its leading cause is the aberrant activation of allergen-specific T helper 2 (Th2) cells (Ballesteros-Tato et al., 2016; Leomicronn, 2017; Leon and Ballesteros-Tato, 2021). The initial priming (or “sensitization”) of allergen-specific CD4^+ T cells is influenced by the interplay between exposures to aeroallergens and their natural content in microbial products (Bachus et al., 2019; Eder et al., 2004, 2005; Eisenbarth et al., 2002; Hammad et al., 2009; Vercelli, 2008; Wilson et al., 2012). Particularly, allergens, such as house dust mites (HDM), are often contaminated with lipopolysaccharide/endotoxin (LPS), and the contribution of LPS to allergenicity has long been of interest and a topic of many reviews (Eder and von Mutius, 2004; Liu and Leung, 2006; Radon, 2006). Epidemiological studies have shown that house dust endotoxin concentrations correlate inversely with inhalant allergen sensitization (Braun-Fahrlander et al., 1999; Braun-Fahrlander et al., 2002; Gehring et al., 2002; Gereda

et al., 2001; Gereda et al., 2000; Stein et al., 2016; von Mutius et al., 2000). These data are consistent with the “hygiene hypothesis” that links low environmental endotoxin exposure to allergy and asthma development. Laboratory mechanistic studies indicate that exposure to airborne allergens containing endotoxin protected against experimental asthma by inducing interleukin-12 (IL-12) production by antigen-presenting dendritic cells (DCs), which led to the suppression of the Th2 cell differentiation program in allergen-specific T cells (Bachus et al., 2019; Bortolatto et al., 2008). However, other studies have shown that LPS could favor sensitization to inhalant allergens by promoting the activation of the airway epithelium and subsequent activation of DCs for Th2 cell priming (Eisenbarth et al., 2002; Hammad et al., 2009; McAlees et al., 2015; Tan et al., 2010). It has been proposed that the LPS dose may be the main cause of this opposite outcome (Kim et al., 2007). However, the same amounts of LPS could either induce or suppress Th2 cell responses in different allergic airway disease models (Bortolatto et al., 2008; Delayre-Orthez et al., 2004; Eisenbarth et al., 2002; Kim et al., 2007), with no clue for this different outcome, and further questioning a dose-dependent mechanism.

Classical migratory DCs (mDCs) play an essential role in activating naive T cells in the draining lymph node (LN). Specifically, mDC2s can promote or suppress Th2 cell responses to aeroallergens depending on their activation status (Bachus et al., 2019; Plantinga et al., 2013), whereas conventional type 1 DCs (cDC1s) poorly acquire allergen-derived antigens and play a minor role (Bachus et al., 2019). Besides, monocyte-derived DCs (moDCs) are greatly induced in the lungs of mice treated with allergens (Plantinga et al., 2013). However, their capacity to migrate to the LN and activate naive T cells is limited (Bachus et al., 2019; Nakano et al., 2013) and, as such, a clear role for these cells has not been established. moDCs are derived from short-lived classical Ly6C^{hi} monocytes during inflammation, but Ly6C^{hi} monocytes can also give rise to non-classical Ly6C^{lo} monocytes during steady state (Gamrekelashvili et al., 2016; Sunderkotter et al., 2004; Varol et al., 2007; Yona et al., 2013). Ly6C^{lo} monocytes are generally considered to have anti-inflammatory activities (Carlin et al., 2013; Quintar et al., 2017), but have also been shown to contribute to inflammation in specific settings (Narasimhan et al., 2019).

Here, we unravel the underlying mechanism of the dual effect of LPS in the priming of allergen-specific Th2 cell responses. We demonstrate that granulocyte-macrophage colony-stimulating factor (GM-CSF) segregates these opposite roles of LPS. In the presence of GM-CSF, *de novo* induced moDCs essentially contributed to LPS-driven protection from allergic inflammation by promoting IL-12 production by antigen-presenting, lung mDC2s. Importantly, GM-CSF-dependent programming enhanced Toll-like receptor 4 (TLR4) expression and intracellular signaling in moDCs and rendered them highly sensitive to low-endotoxin allergen sensitization. Otherwise, in the absence of GM-CSF, low LPS exposure during sensitization did enhance Th2 cell differentiation due to the lack of moDCs. The cysteine protease activity of HDM allergens was found to be essential for GM-CSF production, which was mainly released from non-classical Ly6C^{lo} monocytes. Thus, depletion of non-classical Ly6C^{lo} monocytes or inactivation of cysteine protease activity in HDM allergens abrogated the suppressive function of LPS in Th2 cell response due to the lack of GM-CSF.

Collectively, our data demonstrated that LPS could either promote or prevent Th2-dependent allergic responses depending on the availability of GM-CSF. Besides, our data define the specific roles of classical and non-classical monocytes in this process. Understanding how GM-CSF and LPS-TLR4 orchestrate allergic sensitization may offer new strategies to control allergic airway disease.

RESULTS

LPS inhibits Th2 cell-mediated immunity to inhaled HDM by targeting the hematopoietic compartment

HDM sensitization and challenge (Figure S1A) induced robust Th2-type inflammation, including lung accumulation of Th2 cells and eosinophils, and a rise in HDM-specific serum immunoglobulin E (IgE) levels (Figures S1B-S1H). All these parameters were partially prevented by sensitization with HDM containing 10 ng of LPS, whereas sensitization in the presence of higher doses (100 ng of LPS) completely suppressed Th2-type inflammation (Figures S1B-S1H). No differences were observed in lung neutrophils or monocytes (Figures S1I-S1K). To analyze T cell priming in the lung-draining mediastinal LN (mLN), we transferred 4get.OT-II TCR-transgenic CD4⁺ T cells from naive mice into congenic recipients. Recipients were then sensitized with HDM + ovalbumin (OVA) ± LPS and donor OT-II cells were analyzed for the expression of GFP-IL-4 (Figures S1L-S1O). All doses of LPS prevented the accumulation of GFP⁺4get.OT-II cells, 100 ng LPS doses being more efficient (Figures S1L-S1O). Since 100 ng was the minimum sufficient LPS dose to completely inhibit allergen-specific Th2 cell priming, this dose was selected in subsequent experiments. B6 background was used in the present studies, which displayed optimal priming of Th2 cells after sensitization for 3 consecutive days and a greater response to LPS compared with BALB/c mice (Figure S2).

We next evaluated whether the inhibitory role for LPS was mediated by radioresistant or hematopoietic cells. B6 (wild-type [WT]) or *Tlr4*^{-/-} recipients were irradiated and reconstituted with bone marrow (BM) from WT or *Tlr4*^{-/-} mice. Chimeric mice were then sensitized with HDM ± LPS and challenged with HDM. As expected, HDM sensitization and challenge induced accumulation of Th2 cells (Figures 1A-1C) and eosinophils (Figures 1D-1F) in the lungs of WT recipients reconstituted with WT BM (WT>WT) and, likewise, prompted elevation in the levels of allergen-specific IgE (Figure 1G). Surprisingly, the same results were observed in HDM-treated *Tlr4*[>]*Tlr4* mice, suggesting that our HDM extract does not stimulate TLR4 signaling to promote Th2 cell inflammatory response. As expected, HDM + LPS sensitization prevented the lung accumulation of IL-13⁺IL-5⁺ CD4⁺ Th2 cells (Figures 1A-1C) and eosinophils (Figures 1D-1F), and the induction of specific IgE (Figure 1G) in WT>WT, but not in *Tlr4*[>]*Tlr4* mice. Importantly, prevention of Th2-type lung inflammation was similarly achieved in HDM + LPS-sensitized WT>*Tlr4* but not *Tlr4*[>]WT (Figures 1A-1G), suggesting that the hematopoietic compartment principally contributes to the LPS-induced suppression of Th2-type airway inflammation.

LPS does not directly activate cDC2s but directly stimulates monocytes and moDCs to produce inflammatory cytokines

IL-12 plays an important role in preventing Th2 cell development by promoting T-bet in responding T cells (Bachus et al., 2019). To test whether IL-12 production by DCs was required to suppress Th2 cell priming, we generated BM chimeras that expressed IL-12 normally (DC-WT) or that were selectively IL-12 deficient in CD11c⁺ DCs after diphtheria toxin (DT) administration (DC-IL-12) (Figure S3A) (Leon et al., 2012). We transferred 4get.OT-II CD4⁺ T cells into the chimeras and sensitized and treated them with DT (Figure S3B). Sensitization in the presence of LPS prevented IL-4-GFP in OT-II from DC-WT chimeras, but not in DC-IL-12 chimeras (Figures S3C-S3E). Thus, IL-12 production by CD11c⁺ DCs is required for suppressing Th2 cell priming. HDM + LPS sensitization triggers IL-12 production in allergen-bearing mDC2s (Bachus et al., 2019). Thus, we evaluated whether mDC2s directly responded to LPS to produce IL-12. WT(CD45.1⁺):*Thr4*^{-/-}(CD45.2⁺) mixed BM chimeras (Figure S3F) were sensitized. As expected, HDM + LPS sensitization induced IL-12 production by mLN mDC2s but, importantly, mDC2s from both compartments, WT and *Thr4*^{-/-}, equally produced IL-12 (Figures S3G-S3H), suggesting that LPS did not directly activate mDC2s to promote IL-12. These data were not surprising, since previous results from our lab demonstrated that HDM + LPS sensitization induces indirect activation of mDC2s by LPS-induced tumor necrosis factor α (TNF α) production and TNF α -mediated signaling (Bachus et al., 2019).

We next aimed to characterize cell population(s) in the lung that directly responded to LPS. Sensitization increased the numbers of lung neutrophils (Neu), interstitial macrophages (IM), CD103⁺ mDC1s, CD11b⁺mDC2s, and classical Ly6C^{hi} monocytes (Mo) (Figures 1H and 1I). Importantly, allergen sensitization remarkably induced *de novo* differentiation of Ly6C^{hi}CD64^{hi}CD11b⁺CD11c⁺MHCII⁺ monocyte-derived DCs (moDCs) (Figures 1H and 1I). Otherwise, sensitization did not produce any change in alveolar macrophage (AM) numbers (Figures 1H and 1I). We assessed TNF α production and found that moDCs (and, to a lesser extent, monocytes) are the principal source of TNF α after LPS sensitization (Figures 1J-1K and S4A). We next evaluated whether monocytic cells (i.e., Ly6C^{hi} monocytes and moDCs) directly responded to LPS to produce cytokines. TNF α was induced in Ly6C^{hi} monocytes and moDCs (but not in other lung cell subsets) from chimeras that contained a WT but not a *Thr4*^{-/-} hematopoietic compartment (Figures 1L-1N), suggesting direct activation by LPS through TLR4. Similar results were observed when IL-1 β was analyzed (Figures S4B-S4D). To confirm these data, we used control WT(CD45.1⁺):WT(CD45.2⁺) and experimental WT(CD45.1⁺):*Thr4*^{-/-}(CD45.2⁺) mixed BM chimeras (Figure 1O). As expected, HDM + LPS sensitization induced TNF α (and IL-1 β) production in Ly6C^{hi} monocytes and moDCs but, importantly, cytokine-positive cells were principally restricted to the WT compartment (Figures 1P, 1Q, and S4E-S4G). Overall, the data suggested that the activation of mDC2s for Th2 cell suppression in response to HDM + LPS sensitization is indirectly mediated by cytokines (particularly TNF α [Bachus et al., 2019]) that are released by Ly6C^{hi} monocytes and moDCs in response to direct LPS recognition.

Ly6C^{hi} monocytes are newly recruited to the lung after allergic sensitization and are required to prevent Th2 cell responses to HDM

We next used *Ccr2*^{-/-} mice to investigate the role of monocytic cells in modulating Th2 cell priming to allergens. We confirmed that *Ccr2*^{-/-} mice exhibited markedly reduced lung recruitment of monocytic cells after sensitization (Figures S5A and S5C) and LPS-driven TNF α response (Figure S5I). However, no differences were observed in lung accumulation of neutrophils, mDCs, and macrophage subsets (Figures S5A-S5H). Next, we transferred 4get.OT-II cells into recipients that were then sensitized (Figures 2A-2F). Although OT-II cells expanded equally in all groups, LPS sensitization prevented the accumulation of GFP-IL-4⁺ OT-II cells in WT but not in *Ccr2*^{-/-} mice (Figures 2A-2D). Additionally, OT-II cells in HDM + LPS-treated WT mice expressed higher T-bet levels than OT-II cells in *Ccr2*^{-/-} recipients (Figures 2E and 2F). Similar results were obtained when blocking the CCL2-CCR2 axis using C-C motif chemokine ligand 2 (CCL2)-neutralizing antibody during sensitization (Figures S5J-S5K and S6A-S6E). Furthermore, anti-CCL2 treatment during sensitization inhibited LPS-mediated suppression of later accumulation of Th2 cells and eosinophils in the lung and subsequent serum-specific IgE allergen challenge (Figures S6F-S6M). These data suggested that monocyte recruitment to the lung during sensitization is required for LPS-driven suppression of Th2-type airway inflammation.

Monocytic cells control the capacity of mDC2s to produce IL-12

We next investigated the role of monocytic cells in modulating mDC behavior. We first analyzed the ability of lung mDC subsets to migrate to the mLN after sensitization with Alexa 647-labeled HDM \pm LPS. HDM-bearing, Alexa 647⁺CD11c⁺ DCs were found to homogeneously express high levels of C-C chemokine receptor 7 (CCR7) and major histocompatibility complex class II (MHCII), but did not express monocytic markers such as Ly6C, CD64, and CX3CR1. Neither did they show positive staining with MAR-1 antibody (Figures 2G and 2H). These data suggested that HDM-bearing DCs migrating from the lung resemble mDCs and that lung monocytic cells do not migrate into the mLN. The vast majority of HDM-bearing DCs were CD11b⁺ mDC2s in all groups, but especially upon HDM + LPS sensitization (Figure 2I). Moreover, the frequency and number of HDM-bearing DCs were identical in WT and *Ccr2*^{-/-} mice (Figures 2J-2L). Similar results were obtained when total mDC subsets were analyzed (Figures S7A-S7D). These data show that defective recruitment of monocytes did not affect the number or the capacity of mDC subsets to capture and transport HDM-derived antigens into the mLN.

We next determined the functional capacity of mDCs. Sensitization in the presence of LPS promoted IL-12p70 production by mDC2s from WT but not *Ccr2*^{-/-} mice (Figures 2M-2O). The same treatment also induced T-bet expression in mDC2s from WT but not *Ccr2*^{-/-} mice (Figures 2P and 2Q). Similar results were obtained using CCL2-neutralizing antibody (Figures S7E-S7I). These data suggested that monocytic cells activated in response to LPS control the expression of T-bet in mDC2s, which we formerly found was intrinsically required for the capacity of these cells to produce sustained IL-12 (Bachus et al., 2019). Lastly, we tested the ability of mDCs from HDM + OVA \pm LPS-treated WT and *Ccr2*^{-/-} mice to activate and polarize naive CD4⁺ T cells. mLN CD11c⁺ mDCs were co-cultured with CellTrace Violet (CTV)-labeled naive 4get.OT-II cells. OT-II proliferated equally well

in all conditions (Figure 2R). However, only CD11c⁺ mDCs from HDM + OVA + LPS-sensitized WT mice, but not from *Ccr2*^{-/-} mice, suppressed IL-4-GFP expression in OT-II cells (Figure 2S). No differences were observed in interferon- γ (IFN γ) or IL-2 production by OT-II cells (Figures S7J-S7K). These data suggest that monocytic cells control the capacity of mDCs to prevent Th2 cell priming in responding T cells.

LPS-responding monocytic cells control the activation of mDC2s and thus indirectly suppress Th2 cell priming to HDM

To firmly confirm the role of monocytic cells as primary sensor cells for endotoxin-containing allergens, we generated BM chimeric mice in which cells derived from recruited Ly6C^{hi} monocytes selectively lacked TLR4. Thus, irradiated B6 mice were reconstituted with a mix of *Ccr2*^{-/-} and *Tlr4*^{-/-} BM (mo-TLR4). Control groups were reconstituted with *Ccr2*^{-/-} and WT BM (mo-WT) or WT and *Tlr4*^{-/-} BM (20% TLR4) (Figure 3A). Sensitization in all these chimeric mice induced a similar accumulation of monocytic cells in the lung (Figures S8A and S8B); however, those in mo-TLR4 mice lacked expression of CD284/TLR4 (Figure S8C). Defective TLR4 expression in monocytic cells from mo-TLR4 chimeras did not affect the accumulation of neutrophils and mDC subsets in the lung (Figures S8D-S8G), total numbers of mDC subsets in the mLNs (Figures S8H-S8K), or frequency and number of HDM-bearing, Alexa 647⁺ mDC subsets migrating to the mLN (Figures S8L-S8P). We next sensitized and challenged mo-TLR4 and control chimeras (Figure 3B). Th2 cells (Figures 3C-3E) and eosinophils (Figures 3F-3H) failed to accumulate in the lung of mo-WT and 20% TLR4 control chimeras that were sensitized with HDM + LPS. Importantly, however, LPS exposure was unable to prevent the expansion of Th2 cells (Figures 3C-3E) and eosinophils (Figures 3F-3H) in mo-TLR4 experimental mice. Furthermore, specific IgE responses were suppressed in HDM + LPS-treated control but not mo-TLR4 chimeras (Figure 3I). Additionally, 4get.OT-II cells were transferred into either mo-TLR4 or control mice. Recipients were then sensitized and challenged (Figures S9A-S9E). Again, in mo-TLR4 experimental mice, LPS exposure failed to prevent the lung accumulation of Th2 cells (either derived from donor OT-II [Figures S9D-S9E] or endogenous [Figures S9B and S9C] CD4⁺ T cells). However, importantly, intranasal (i.n.) instillation of *in vitro* generated WT mo-DCs (but not TLR4^{-/-} mo-DCs) at the time of sensitization restored the WT phenotype in mo-TLR4 chimeras, including the prevention of donor and endogenous Th2 cell accumulation in the lung (Figures S9A-S9E), the inhibition of lung eosinophilia (Figures S9F-S9H), and the suppression of serum-specific IgE (Figure S9I). These data suggest that monocytic cells responding to LPS, and most particularly moDCs, govern the suppression of Th2-type allergic airway inflammation.

Next, we tested whether impaired LPS signaling in monocytic cells affected the initial priming of specific T cells (Figure 3J). LPS treatment could not prevent the accumulation of donor-derived GFP-IL-4⁺ OT-II cells in mo-TLR4 chimeras, as it did in control chimeras (Figures 3K-3N). However, i.n. delivery of WT moDCs in HDM + LPS-treated mo-TLR4 mice was sufficient to prevent the accumulation of GFP⁺OT-II cells (Figures S9J-S9M). Thus, LPS-responsive monocytic cells/moDCs are required to suppress the priming of allergen-specific Th2 cell responses to allergens harboring endotoxin. Using chimeric mice in which cells derived from recruited Ly6C^{hi} monocytes selectively lacked the ability

to produce TNF α (mo-TNF α) further showed that LPS-driven production of TNF α by monocytic cells was required to prevent Th2 cell priming (Figures S9N-S9Q).

Finally, we tested the functional ability of mDCs in mo-TLR4 chimeras. We purified mLN mDCs from sensitized mice and co-cultured them with naive 4get.OT-II cells. OT-II proliferated equally (Figure 3O). Only those stimulated with mDCs from HDM + OVA + LPS-sensitized mo-WT mice, but not from mo-TLR4 mice, suppressed IL-4-GFP expression (Figure 3P). No differences were observed in IFN γ or IL-2 production by OT-II cells (Figures S9R and S9S). Furthermore, we found that mDC2s from HDM + LPS-treated mo-TLR4 mice displayed defective ability to express T-bet (Figures 3Q and 3R) and produce IL-12p70 (Figures 3S and 3U) compared with control chimeras. However, i.n. delivery of WT moDCs was able to restore a phenotype similar to the one shown in control mice (Figures S9T and S9U). Collectively, these data suggest that moDCs newly formed from recruited Ly6C^{hi} monocytes efficiently sense and respond to endotoxin contained in aeroallergens. By doing so, moDCs control the ability of mDC2 to produce IL-12 and, hence, the capacity of mDC2s to prevent Th2 cell priming to allergens.

GM-CSF signaling is required to prevent Th2 cell responses to HDM

moDCs are traditionally generated from monocytes by *in vitro* treatment with GM-CSF. Thus, we first tested whether HDM sensitization induced moDC differentiation in a GM-CSF-dependent manner. Treatment with anti-GM-CSF neutralizing antibody at the time of sensitization did not alter the frequency or total number of monocytic cells (CD11b⁺Ly6C^{hi}) infiltrating the lungs, but it did prevent the differentiation of CD11c⁺MHCII⁺CD64^{hi} moDCs (Figures 4A and 4B). We further found that anti-GM-CSF treatment also abrogated TNF α production after HDM + LPS sensitization (Figures 4C and 4D). These data indicate that GM-CSF induced monocytes to differentiate into moDCs and also boosted their ability to respond to LPS.

To investigate the mechanisms by which GM-CSF can enhance LPS responsiveness in monocytes, we sorted BM monocytes, stimulated them with PBS (Ctrl) or GM-CSF for 3 h, and performed RNA sequencing (RNA-seq). More than 2,400 genes were differentially expressed between Ctrl and GM-CSF-treated monocytes (Figure 4E and Table S1). Interestingly, a significant number of transcripts related to TLR-mediated TIRAP-MyD88-dependent signaling pathway, regulating early nuclear factor- κ B and activator protein-1 activation and associated inflammatory cytokine production such as TNF α , were highly expressed in GM-CSF-treated relative to Ctrl monocytes (Figure 4E). Conversely, we found transcripts related to type-I IFN production and signaling, including many related to TLR-mediated TRIF-TRAM pathway, were otherwise downregulated in GM-CSF-treated relative to Ctrl monocytes (Figure 4E). In agreement, gene set enrichment analysis (GSEA) revealed that the transcriptome of GM-CSF-treated monocytes was significantly enriched relative to the Ctrl transcriptome in genes involved in the superpathway network for activated TLR4 signaling (Figure 4F). Instead, the opposite was observed when the analysis was done with a defined set of genes implicated in the superpathway network for IFN α / β signaling (Figure 4G). These data suggested that GM-CSF could prime monocytes for LPS responsiveness by enhancing TLR4 expression and intracellular signaling. To better understand this effect,

we stimulated fresh purified BM monocytes with different doses of LPS in the presence or absence of GM-CSF. Additionally, purified monocytes were cultured in the presence of GM-CSF for 3 h or 24 h and then stimulated with different doses of LPS. In all the conditions, cells were analyzed for surface markers (Figure 4H) and intracellular TNF α production (Figures 4I and S10A) after 2.5 h of LPS stimulation. Since 24-h GM-CSF pre-treatment induced differentiation of the majority fraction of monocytes into CD11c⁺MHCII⁺ moDCs (Figure 4H), the analysis was separately performed in monocyte-like and moDC-like phenotypes. We found that GM-CSF pre-treatment (either 3 h or 24 h) enhanced the ability of monocyte-like cells to produce TNF α in response to lower concentrations of LPS (Figures 4I and S10A). However, moDCs showed the greatest capacity to produce TNF α even at very low LPS concentrations (Figures 4I and S10A). These data suggest that GM-CSF induces moDC differentiation but further empowers these cells to sense and react to very low levels of LPS.

Next, we wanted to determine the effect of GM-CSF neutralization during sensitization on mDC2 function. No differences between anti-GM-CSF-treated and Ctrl mice were found in the frequency and number of mDC subsets in the lung (Figures S10B and S10C) or mLN (data not shown). However, we found that GM-CSF neutralization impaired the IL-12-producing capacity of mDC2s from HDM + LPS-treated mice (Figures 4J and 4K), which correlated with the blockade of TNF α secretion by monocytic cells in these mice (Figures 4C and 4D). Furthermore, we found that GM-CSF neutralization during HDM + LPS sensitization abolished the suppressive effect of LPS on Th2 cell accumulation in the lungs (Figures 4L-4N). Of note, although GM-CSF neutralization partially reduced neutrophil numbers in the lungs (Figures S10D and S10E), Ly6G-mediated neutrophil depletion did not affect the suppression of Th2 cell responses by LPS (Figures S10F-S10J). Thus, our data indicate that GM-CSF availability underpins LPS-mediated suppression of Th2 cell responses to HDM.

GM-CSF availability governs the ability of LPS to suppress Th2 cell responses to aeroallergens

OVA is frequently used as an aeroallergen to induce Th2-type airway inflammation in animal models. Although high doses of LPS (~10 μ g) always prevent allergic inflammation, the presence of low-dose LPS (0.1 μ g) in OVA preparations is necessary to induce Th2 cell responses to inhaled OVA, which otherwise behaves as an inert antigen (Eisenbarth et al., 2002; Kim et al., 2007). Curiously, the same low amounts of LPS (0.1 μ g) have the opposite outcome in our HDM-induced model of allergic inflammation. Since our data suggest that GM-CSF can influence host sensitivity to LPS, we wanted to test whether different results seen with OVA + LPS and HDM + LPS protocols were due to the different ability of OVA and HDM to elicit GM-CSF production. Thus, we first determined GM-CSF response in bronchoalveolar lavage (BAL) fluid from mice sensitized with HDM or OVA \pm LPS. HDM sensitization caused a great increase in GM-CSF compared with OVA, independently of the presence of LPS (Figure 5A). Accordingly, OVA \pm LPS-sensitized mice did not show substantial monocyte differentiation into moDC (Figures 5B and 5C) nor a manifest capacity of these cells to produce TNF α (Figures 5D and 5E). However, the co-administration of GM-CSF enhanced moDC differentiation (Figures 5B and 5C) and TNF α production

in OVA + LPS-treated mice (Figures 5D and 5E). Thus, GM-CSF can potentiate the LPS-induced cytokine response in monocytic cells from OVA + LPS-sensitized mice.

We next test whether this effect can influence OVA + LPS-driven Th2 development. We first investigated the dynamics and Th2 cell polarizing functions of mDC2s. We found that sensitization with OVA alone did not cause an important accumulation of mDC2s in the lung (Figure S11A) nor induced relevant migration of mDC2s into the mLN (Figure S11B). However, co-administration of GM-CSF or LPS greatly increased lung accumulation and mLN migration of mDC2s (Figures S11A and S11B). This effect was not affected by the inhibition of monocyte recruitment to the lung with CCL2-neutralizing antibody (Figure S11B). Although OVA + LPS sensitization did not stimulate IL-12p70 production by mDC2s, GM-CSF co-administration did induce IL-12p70 production by mDC2s (Figures 5F and 5G). Importantly, CCL2 neutralization during GM-CSF + OVA + LPS sensitization abolished the enhanced effect of GM-CSF + LPS on IL-12p70 production by mDC2s (Figures 5F and 5G), suggesting that this effect was mediated by monocyte-dependent regulation of mDC2 activation.

We next tested the ability of mDC2s to activate naive CD4⁺ T cells. mLN mDCs were co-cultured with 4get.OT-II cells. OT-II proliferated equally well in all conditions, except when stimulated with mDCs from OVA-sensitized mice (Figure 5H), suggesting that OVA alone did not license the T cell stimulatory capacity of mDCs. OT-II cells primed by mDCs from OVA + GM-CSF and OVA + LPS-sensitized mice induced IL-4-GFP expression (Figure 5I), showing that both *in vivo* treatments (GM-CSF and LPS), when given separately, can stimulate the Th2 cell priming capacity of mDCs. However, combined *in vivo* treatment with OVA + GM-CSF + LPS suppressed the ability of mDCs to induce IL-4-GFP expression in OT-II cells, yet this suppression was abrogated by CCL2 neutralization *in vivo* (Figure 5I). No differences were observed when analyzing IFN γ production by the OT-II cells (Figure S11C). These results indicated that although the presence of low-dose LPS or GM-CSF, together with an antigen, could stimulate mDC2s to prime Th2 cells, the concurrence of both low-dose LPS and GM-CSF efficiently enabled IL-12 secretion in mDC2s, hence their ability to suppress Th2 cell priming. Our data further suggest that the acquisition of this capacity in mDC2s was mediated by activation of monocytic cells that had been programmed by GM-CSF to efficiently sense and react to low-dose LPS.

We next evaluated *in vivo* OVA-specific T cell responses. Although either GM-CSF or LPS induced expansion and IL-4-GFP expression in donor OT-II cells, a combination of both treatments prevented IL-4-GFP expression in OT-II cells (Figures 5J-5M). By contrast, CCL2 neutralization abrogated the effect of combined GM-CSF + LPS sensitization (Figures 5J-5M). Post-challenge analysis showed that either GM-CSF or LPS sensitization promoted lung accumulation of Th2 cells compared with OVA alone, and endogenous CCL2 neutralization did not affect this outcome (Figures 5N-5P and data not shown). Importantly, sensitization with both GM-CSF + LPS prevented the accumulation of Th2 cells, but in this case endogenous CCL2 neutralization did abolish this effect. Furthermore, *in vitro* GM-CSF-generated moDCs was sufficient to prevent the accumulation of Th2 cells in LPS-sensitized mice (Figures 5N-5P). These data indicated that the programming of Ly6C^{hi} monocytes by GM-CSF essentially contributes to prevent Th2 cell differentiation in

response to allergens that contain endotoxin and may suggest that the nature of the allergen determines the availability of GM-CSF.

Non-classical Ly6C^{lo} monocytes produce GM-CSF after HDM sensitization

We next evaluated whether GM-CSF was produced by radioresistant or hematopoietic cells in the lungs. Mice were reconstituted with BM from WT (WT-WT) or GM-CSF-deficient *Csf2*^{-/-} (GM-WT) mice (Figure 6A). Mice were then transferred with 4get.OT-II cells and sensitized in the presence or absence of anti-GM-CSF neutralizing antibody (Figure 6B). Sensitization in the presence of LPS prevented IL-4-GFP in WT-WT but not in GM-WT chimeras or in mice treated with anti-GM-CSF neutralizing antibody (Figures 6C-6F). GM-WT chimeras also showed defective differentiation of CD11c⁺CD64^{hi} moDCs after sensitization, similar to anti-GM-CSF treatment (Figures S12A and S12B). These data suggest that radiosensitive BM-derived cells were a needed source of GM-CSF.

We next characterized GM-CSF-producing cells in WT(CD45.1⁺) recipient chimeras reconstituted with WT(CD45.2⁺) BM (Figures 6G and S12B-S12F). First, we found that ~40% of CD3⁺CD90⁺ T cells and Lin⁻CD127⁺CD90⁺ innate lymphoid cells in lung cell suspensions were radioresistant/recipient-derived, i.e., CD45.1⁺ (Figure S12C); whereas monocyte subsets, neutrophils, eosinophils, AM, IM, and mDCs were found to be CD45.2⁺ BM-derived (>99%) (data not shown). GM-CSF expression was detected by intracellular staining after sensitization in lung CD45.2⁺ BM-derived cells (Figure 6G). GM-CSF⁺ cells did not express CD3 and CD90 but expressed the macrophage/monocyte markers CD11b, F4/80, CD115, and CX3CR1 (Figure 6G). They did not express MHCII, and expressed only low levels of Ly6C and CD64 and intermediate levels of CD11c (Figure 6G). They also showed MAR-1 staining (Figure 6G) and a low side scatter (SSC) profile (data not shown). This phenotype closely resembles that described for non-classical monocytes (Geissmann et al., 2003; Sunderkotter et al., 2004). We next characterized non-classical monocytes in relation to other radiosensitive lung cells, including Ly6C^{hi} monocytic cells, AM, IM, eosinophils, and mDC2s (Figure S12D), and monocyte subsets in the blood (Figure S12E). We defined non-classical monocytes as Ly6C^{lo}CD11b⁺CD64^{lo}Siglec-F⁻F4/80⁺MAR-1⁺CCR2⁻CD117^{int}CD115⁺MertK⁻CX3CR1^{hi}CD11c⁺MHCII⁻CD16.2^{hi}CD62L⁻SSC^{lo} cells, both in the lung (Figures S12D and S12G) and blood (Figures S12E and S12G). Non-classical monocytes were also CD90⁻ and CD49b⁻ (data not shown). Although we found non-classical monocytes were MAR-1⁺CD117^{int}, they were different from mast cells (MCs), since those expressed high levels of CD117 but not CD11b and F4/80 (Figure S12F). MCs were also SSC^{hi} and radioresistant/recipient-derived CD45.1⁺ cells (Figure S12F). Furthermore, MCs were absent in c-Kit^{w-sh} mice, but non-classical monocytes were not affected (data not shown). Sensitization did not produce any change in non-classical monocyte numbers in the lung, nor did the lack of CCR2 expression (Figure S12H), while both affected the recruitment of classical Ly6C^{hi} monocytes (Figure S12I). Overall, these analyses identify that GM-CSF-producing cells in sensitized lungs corresponded to non-classical Ly6C^{lo} monocytes.

Clodronate liposomes administered intravascularly transiently deplete blood and perivascular populations of monocytes/macrophages. Ly6C^{hi} monocytes rapidly return to

normal levels, whereas non-classical Ly6C^{lo} monocytes have delayed recovery kinetics (Misharin et al., 2014; Olingy et al., 2017; Sunderkotter et al., 2004). Intravascular CD45 staining indicated that non-classical Ly6C^{lo} monocytes have a perivascular location in the lung (Figure S13A), as others have described (Auffray et al., 2007; Olingy et al., 2017). Classical and non-classical monocytes were depleted at 16 h after a single intraventricular (i.v.) injection of clodronate liposomes (data not shown). Two days after i.v. clodronate treatment, a profound depletion of non-classical monocytes was still observed in the lung (Figures 6H and 6J). Subsequent sensitization on day 2 and analysis on day 3 (Figure 6H) showed similar constant depletion of non-classical monocytes in the lung (Figures 6I and 6J) and blood (Figure S13F). Non-classical monocytes returned to normal numbers by day 12 (Figure S13B). Classical monocytes, however, returned to normal levels by day 2. Hence, normal numbers of lung monocytic cells (Ly6C^{hi} monocytes and moDCs) (Figures 6J and S13C-S13E) and blood Ly6C^{hi} monocytes (Figure S13F) were found on day 2 (naive) or day 3 (1 day post-sensitization). i.v. clodronate treatment did not alter the numbers of neutrophils, AM, IM, eosinophils, and mDC subsets in the lung (Figures 6J and S13C-S13E), nor the number of neutrophils and eosinophils in the blood (Figure S13F), whereas intrathecal (i.t.) clodronate treatment affected lung AM but not monocytes (Figure S13C-S13F). i.v. clodronate treatment affected neither the frequency (Figure S13G) nor number (Figure S13H) of HDM-bearing, Alexa 647⁺ mDC2s, and mDC1s migrating into the mLN on day 3. MCs (Figure S13I) and circulating basophils (Figure S13J) were also unaffected. Of note, basophils and non-classical monocytes were both CD11b⁺MAR-1⁺; however, basophils differed from non-classical monocytes as they did not express F4/80, CD11c, or CD117, but expressed intermediate levels of CD90 (Figure S13J).

Since i.v. clodronate efficiently and specifically deleted non-classical monocytes in the lung from day 2, and for a minimum of 4 additional days, we next analyzed its effect on GM-CSF expression. Clodronate treatment suppressed GM-CSF response in BAL fluid (Figure 6K) and the induction of lung GM-CSF⁺ cells (Figures 6L and 6M) after HDM sensitization. This was accompanied by poor moDC differentiation (Figures 6N and 6O) and reduced mo-DC-derived TNF α response after HDM + LPS sensitization (Figure 6P). These defects were reversed with co-administration of GM-CSF (Figures 6N and 6O; data not shown). i.t. clodronate treatment, however, had no effect on GM-CSF/moDC response (data not shown).

We next tested whether clodronate-induced depletion of non-classical monocytes affected Th2 cell responses. Although donor OT-II cells expanded equally, LPS sensitization prevented the accumulation of GFP⁺ OT-II cells in control mice but not in clodronate-treated mice (Figures 6R-6U). Furthermore, clodronate treatment during sensitization inhibited LPS-mediated suppression of post-challenge accumulation of Th2 cells in the lung (Figures S13K-S13L). GM-CSF co-treatment was sufficient to prevent the accumulation of Th2 cells in clodronate-treated LPS-sensitized mice (Figures 6R-U and S13K-S13L). These data indicated that non-classical Ly6C^{lo} monocytes produce GM-CSF after HDM sensitization and thus contribute to the programming of Ly6C^{hi} monocytes for LPS-induced suppression of allergic Th2 cell responses.

HDM with cysteine protease activity induces GM-CSF production

We next explored whether different allergens induce GM-CSF production. Sensitization with HDM or with the protease allergen papain caused a significant increase in GM-CSF, whereas German cockroach sensitization did not (Figure 7A). Accordingly, whereas HDM and papain sensitization caused moDC differentiation, cockroach sensitization failed to induce moDCs (Figures 7B and 7C).

Since papain and cockroach allergens induced different GM-CSF and moDC responses, we next analyzed its effect on LPS-driven Th2 development. As expected, LPS inhibited the priming of donor IL-4⁺GFP⁺ OT-II cells in papain sensitized mice (Figures S14A-S14D) and post-challenge accumulation of Th2 cells (Figures S14H-S14I) and eosinophils (Figures S14K-S14L) in the lung. GM-CSF neutralization, however, abolished this suppressive effect of LPS (Figures S14A-S14D). In contrast, LPS sensitization did not have effect in cockroach-treated mice (Figures S14A-S14M).

Since the nature of the allergen seems to determine GM-CSF production, we explored whether enzymatic activities in allergens play a role. Papain is a cysteine protease. HDM extracts contain group 1 allergens with cysteine protease, papain-like activity (Reithofer and Jahn-Schmid, 2017). Conversely, cysteinelike proteases have not been identified in extracts from German cockroach (Polley et al., 2017) nor do they show cysteine protease activity *in vivo* (Bhat et al., 2003; Page et al., 2010). Thus, HDM was heat-inactivated or treated with irreversible inhibitors of cysteine (E-64) or serine (4-(2-aminoethyl)-benzenesulfonyl fluoride [AEBSF]) protease activities. Heat-induced inactivation or treatment with E-64 prevented GM-CSF response after HDM sensitization, as indicated by the measurement of cytokine levels in BAL fluid (Figure 7D) and GM-CSF production by non-classical Ly6C^{lo} monocytes (Figures 7E and 7F). However, GM-CSF response was unaffected by the inactivation of serine proteases with AEBSF inhibitor (Figures 7D-7F). No effect was found either after sensitization with HDM treated with chitinase or β -glucanase (data not shown). Furthermore, no effect was found if E-64 and HDM were not pre-incubated before administration (data not shown). Inactivation of protease activity of HDM did not affect the ability of lung cells to take HDM (Figure S14N) or the capacity of mDC subsets to capture and transport HDM-derived antigens into the mLN (Figures S14O-S14R). As a control, inactivation of protease activity of papain inhibited the acquisition of allergen by mDCs (Figures S14N and S14O). These data indicated that cysteine protease activity in HDM triggers GM-CSF production by non-classical Ly6C^{lo} monocytes. No cytokine response was found in Ly6C^{lo} monocytes after direct HDM stimulation, suggesting indirect activation (Figure S14S).

We next explored whether the inactivation of cysteine protease activity of HDM affected moDC differentiation and Th2 cell responses. Heat-induced inactivation or E-64 treatment, but not AEBSF treatment, prevented moDC differentiation after sensitization (Figures 7G and 7H). Accordingly, heat-induced inactivation or E-64 treatment abolished the suppressive effect of LPS on Th2 cell responses, including the priming of IL-4⁺ T cells in the mLN after sensitization (Figures 7I-7L) and the accumulation of IL-13⁺IL-5⁺ Th2 cells in the lung after challenge (Figures S14T-S14V). Importantly, sensitization in the presence of GM-CSF

restored the capacity of LPS to prevent Th2 cell responses in these mice (Figures 7I-7L and S14T-S14V).

Collectively, our data indicate that cysteine protease activity in allergens triggers GM-CSF production by non-classical Ly6C^{lo} monocytes in the lung. Subsequently, the programming of classical Ly6C^{hi} monocytes by GM-CSF essentially contributes to prevent Th2 cell differentiation in response to allergens containing endotoxin. GM-CSF priming leads the differentiation of Ly6C^{hi} monocytes into mDCs with enhanced capacity to sense low-dose LPS and produce large quantities of pro-inflammatory cytokines, particularly TNF α . Enhanced LPS-dependent activation in GM-CSF-primed Ly6C^{hi} monocytes regulates the IL-12-producing ability of mDC2s and, thereby, impedes Th2 cell differentiation in response to low-endotoxin allergen sensitization.

DISCUSSION

The relationship between allergen sensitization and endotoxin exposure is complex. Whereas many studies have found that exposure to endotoxin protects against allergen sensitization and asthma development (Braun-Fahrlander et al., 1999; Braun-Fahrlander et al., 2002; Gehring et al., 2002; Gereda et al., 2001; Gereda et al., 2000; Stein et al., 2016; von Mutius et al., 2000), other studies have found that endotoxin levels positively correlate with sensitization to inhalant allergens, especially in individuals with a genetic predisposition (Bolte et al., 2003; Celedon et al., 2007). Furthermore, gene variations in LPS signal transducers are sometimes, but not always, associated with increased sensitization, suggesting that other factors can modify the predisposition to allergic disease (Medvedev, 2013; Vercelli, 2008). The mechanisms underlying these contradictory conclusions are still obscure.

Previous animal studies have shown that LPS can either promote or prevent allergic sensitization when present in allergens (Bachus et al., 2019; Bortolatto et al., 2008; Delayre-Orthez et al., 2004; Eisenbarth et al., 2002; Kim et al., 2007; McAlees et al., 2015; Tan et al., 2010). Although the amount of LPS can be critical in determining these opposite outcomes, with low-dose LPS promoting and high-dose LPS preventing sensitization, the LPS doses that consistently cause the same expected effects across the different animal models have not yet been defined. For example, a 10- to 100-ng dose of LPS was required to stimulate Th2 cell responses and achieve allergic sensitization to inhaled OVA (Eisenbarth et al., 2002; Kim et al., 2007). In contrast, the same amounts of LPS prevented allergic sensitization in our HDM murine model. Others have similarly observed that sensitization in the presence of low-dose LPS (10–100 ng) prevented, rather than promoted, Th2-mediated allergic responses in other murine models (Bortolatto et al., 2008; Delayre-Orthez et al., 2004). Therefore, the differential roles of LPS in Th2 cell development cannot merely be explained by a dose-dependent mechanism.

Various studies have demonstrated that LPS-driven stimulation of TLR4 on different compartments controlled distinct functions of LPS on allergen-specific T cell responses. Specifically, LPS-driven stimulation on airway epithelial cells was found to be important for LPS-enhanced Th2 cell responses to inhaled allergens, by stimulating the production of pro-

allergic cytokines and the consequent activation and migration of antigen-containing DCs (Eisenbarth et al., 2002; Hammad et al., 2009; Leomicronn, 2017; McAlees et al., 2015; Tan et al., 2010). Our data, however, showed that LPS-driven activation is not essentially required to induce Th2 cell sensitization to HDM allergens. Relatedly, data from previous studies have suggested that LPS content can contribute to Th2 cell priming in HDM extracts that have a poor capacity to promote Th2 cell differentiation. Still, it is dispensable for HDM extracts that induce robust Th2 cell responses (Wilson et al., 2012). In this regard, HDM extracts can largely vary in their content of various TLR ligands and glycosylated motifs (Gandhi and Vliagoftis, 2015; Nathan et al., 2009; Ryu et al., 2013; Wilson et al., 2012), which can have overlapping functions in inducing the activation and migration of antigen-containing DCs (Leomicronn, 2017).

Conversely, LPS-induced TLR4 activation in hematopoietic cells seemed to be most involved in the induction of Th1/Th17 cell responses to allergens (McAlees et al., 2015; Tan et al., 2010). Here we show that LPS-driven stimulation of the hematopoietic compartment is needed to suppress Th2 cell sensitization to HDM. Our previous data have demonstrated that mDC2s are the principal DC subset that captures and transports HDM-derived antigens from the lung into the mLN; furthermore, they are the dominant IL-12-producing DC subset in the mLN, and hence are the main drivers preventing allergic Th2 cell responses in HDM + LPS-sensitized mice (Bachus et al., 2019). Here, we show that the ability of mDC2s to produce IL-12 and suppress Th2 cell priming did not require direct recognition of LPS, but instead these functions were controlled by monocytes that activated the differentiation program into moDCs. Notably, the functional programming of moDCs allowed these cells to increase their sensitivity to LPS so that low doses of LPS could then stimulate a different cascade of cytokines in the lung, allowing the indirect activation of lung-migratory DC2s for Th2 cell suppression rather than promotion. Thus, our findings indicate that moDCs have a role as amplifiers and modifiers of LPS functions in allergic inflammation.

We have found that GM-CSF is an important factor controlling the functional programming of moDCs and their subsequent responsiveness to LPS. As such, low-dose LPS can very efficiently target GM-CSF-driven moDCs for Th2 cell suppression; but particularly on the congenic B6 background. Instead, low-dose LPS sensitization in BALB/c mice had no suppressive effects or even potentiated allergen-specific Th2 cell response upon suboptimal allergen sensitization. Others have found that low-dose LPS treatment in BALB/c mice has a pro-allergic effect after subthreshold allergen exposure by potentiating the allergen uptake by DCs (Radermecker et al., 2019). Differential LPS sensitivity in B6 and BALB/c mice has been described, BALB/c mice being a low LPS responder due to a reduced surface expression of TLR4 (Tsukamoto et al., 2013). Thus, the genetic control of LPS responsiveness can also account for important differences in allergic sensitization. Likewise, LPS response also controls allergic sensitization during infancy. We have previously published that LPS hyporesponsiveness in infant mice leads to higher susceptibility to Th2 sensitization (Bachus et al., 2019). Future research will answer whether this is due to different regulation of the GM-CSF-LPS axis and how environmental factors impacting during the infant period can affect these pathways. On the other hand, our and other data support that in the absence of LPS, GM-CSF stimulates mDC2 migration and Th2 cell differentiation, particularly to weak allergens such as OVA (Stampfli et al., 1998),

subthreshold levels of HDM (Llop-Guevara et al., 2014), or cockroach allergens (Sheih et al., 2017). Overall, the interplay between the GM-CSF response elicited after allergen exposure and the amount of endotoxin contained in those inhaled allergens can oppositely balance the activation of mDC2s and, in the end, establish whether the stimulated allergen-specific T cell response will be protective or pathogenic.

Our data show that non-classical Ly6C^{lo} monocytes produce GM-CSF and reveal an additional function of these cells in the context of allergic sensitization. Furthermore, our data show that the cysteine protease activity found in HDM allergens plays a major role in triggering GM-CSF production by non-classical Ly6C^{lo} monocytes. The sensing of allergen-associated protease activity has been proposed to essentially contribute to the initiation of allergic diseases (Cayrol et al., 2018; Perner et al., 2020; Reithofer and Jahn-Schmid, 2017; Serhan et al., 2019). Here we show that it also rules the suppression of allergic sensitization when low amounts of LPS are present in allergens. While HDM did not activate GM-CSF production by non-classical Ly6C^{lo} monocytes *in vitro*, it did so *in vivo*. This might indicate that HDM activates non-classical Ly6C^{lo} monocytes through an indirect mechanism. Cysteine proteases in HDM extracts have been shown to be able to directly stimulate airway epithelial cells (Asokanathan et al., 2002) and sensory neurons (Serhan et al., 2019) by activating protease-activated receptors. However, the cellular interactions required for stimulating GM-CSF response in non-classical Ly6C^{lo} monocytes remain to be elucidated.

In summary, our results show that GM-CSF segregates the opposed functions of LPS in the priming of allergen-specific Th2 cell responses. Different host sensitivities to GM-CSF and/or LPS (influenced by genetic diversity or environmental factors) can therefore significantly affect the risk of allergic sensitization. Understanding these interactions may provide insight into future therapeutic interventions to circumvent and even reverse allergic disease.

Limitations of the study

The experiments of this study use mice that were randomized into groups of 3–6 mice/group/time point. Despite the small sample size, parametric tests were used to detect statistical differences. These tests assume that the data are distributed normally. Although the sample size of individual experiments does not always permit an accurate assessment of normality, our experience with the animal models in this study and with multiple sets of replicates has indicated that the measurements reported in this paper follow a normal distribution and satisfy the requirements for parametric tests. Thus, parametric tests were used because they have greater statistical power to detect existing differences between groups.

STAR★METHODS

RESOURCE AVAILABILITY

Lead contact—Additional information and requests for resources and reagents can be direct to and fulfilled by lead contact, Dr. Beatriz León (bleon@uab.edu).

Materials availability—This paper does not generate unique materials.

Data and code availability—Raw data files and processed sequencing for RNA-Seq analyses reported in this paper have been deposited in the GEO database under the accession code: GSE186449.

This paper does not report original code.

Any additional information required to reanalyze the data reported in this paper is available from the lead contact upon request.

EXPERIMENTAL MODELS AND SUBJECT DETAILS

Mouse strains—The mouse strains used in these experiments include: C57BL/6J (B6), B6.SJL-Ptprca Pepcb/BoyJ (CD45.1⁺ B6 congenic), C57BL/6-Tg(TcraTcrb)425Cbn/J (OT-II), B6.129-II4tm1Lky/J (B6.4get IL-4 reporter mice), C.129-II4tm1Lky/J (BALB/c.4get IL-4 reporter mice), B6(Cg)-Tlr4tm1.2Karp/J (*Tlr4*^{-/-}), B6.129S1-II12atm1Jm/J (*Il12a*^{-/-}), B6.FVB-Tg(Itgax-DTR/EGFP)57Lan/J (Itgax-DTR,-EGFP), B6.129S4-Ccr2tm1Ifc/J (*Ccr2*^{-/-}), BALB/cJ (BALB/c), C.Cg-Tg(DO11.10)10Dlo/J (DO11.10), CBy.PL(B6)-Thy1a/ScrJ (BALB/c Thy1.1⁺), B6.129S-Csf2tm1Mlg/J (*Csf2*^{-/-}), B6; 129S-Tnftm1Gkl/J (*TNFa*^{-/-}), and B6.Cg-KitW-sh/HNihJaeBsmJ (cKitw-sh). B6.4get mice were originally obtained from Dr. M. Mohrs (Trudeau Institute). All other mice were originally obtained from Jackson Laboratory and were bred and housed in the University of Alabama at Birmingham animal facility under specific pathogen-free conditions. Experiments were equally performed with male and female mice and initiated between 8 and 10 weeks of age. The University of Alabama at Birmingham Institutional Animal Care and Use Committee approved all procedures involving animals.

METHOD DETAILS

Immunizations—HDM (*Dermatophagoides pteronyssinus* and *D. farinae*; ~40ug/mg Der p1/f1) and German Cockroach (*Blattella germanica*) extracts were obtained from Greer Laboratories (<12 EU/mg endotoxin). Papain from papaya latex was obtained from Sigma-Aldrich (<0.1 EU/mg endotoxin; 8 U/mg). Mice were intranasally administered (i.n.) with 50 µg of HDM extract, 50 µg of Cockroach extract, or 10 µg of Papain +/- 5 µg of LPS-free EndoFit OVA (<0.1 EU/mg endotoxin; InvivoGen) +/- LPS from *Escherichia coli* 0111:B4 (Sigma-Aldrich) +/- 100 ng of recombinant GM-CSF (PeproTech) +/- 3-5 × 10⁵ *in vitro* GM-CSF-generated moDCs daily for 1-3 days and challenged (i.n.) with 50 µg of HDM, 50 µg of Cockroach extract, or 10 µg of Papain +/- 5 µg of LPS-free EndoFit OVA for 3 days. i.n. administrations were given in 100 µL of PBS. In some experiments, mice were intraperitoneally administered (i.p.) with 250 µg of anti-CCL2 antibody (BioXCell), 200 µg anti-GM-CSF antibody (BioXcell), or 250 µg of anti-Ly6G antibody (BioXCell) at the time of initial sensitization. To deplete CD11c⁺ cells, *Itgax*-DTR BM chimeras were i.p. treated with 60 ng DT (Sigma-Aldrich) on day 3 after sensitization. To deplete non-classical monocytes mice were injected i.v. with a single dose of clodronate liposomes or control liposome suspensions (100 µL/0.5 mg), from Encapsula NanoSciences, 48 h prior sensitization. 50 µL/0.25 mg clodronate liposomes were administered i.t. for

depletion of alveolar macrophages. In some experiments allergen extract was labeled with AF647 labeling kit (Invitrogen) prior to administration to mice. In some experiments HDM or papain were heat-inactivated (100°C for 45 min), treated with the irreversible cysteine protease inhibitor E-64 (100 nM; 37°C for 30 min), the irreversible serine protease inhibitor AEBSF (1 mM; 37°C for 30 minutes), chitinase (1 unit/100ug) or beta-(1->3)-D-Glucanase (1 unit/100ug), all from Sigma-Aldrich. For intra and perivascular staining, mice were i.v. administered anti-CD45.2 antibody clone 104 from BD bioscience (3ug/mice) 5 minutes before they were euthanized and harvested.

BM chimeras—Recipient mice were irradiated with 950 Rads from a high-energy X-rays source delivered in a split dose and reconstituted with 10^7 total BM cells. Mice were allowed to reconstitute for at least 8–12 weeks before HDM treatment.

Cell preparation and flow cytometry—Lungs were isolated, cut into small fragments and digested for 45 min at 37°C with 0.6 mg/mL collagenase A (Sigma) and 30 µg/mL DNase I (Sigma) in RPMI-1640 medium (GIBCO). Digested lungs, mLN or spleens were mechanically disrupted by passage through a wire mesh. Blood was collected in Dextran-EDTA buffer. Peritoneal cells were obtained from lavages with 5–10 mL phosphate buffered saline (PBS) using a 21-G needle. Red blood cells were lysed with 150 mM NH₄Cl, 10 mM KHCO₃ and 0.1 mM EDTA. Fc receptors were blocked with anti-mouse CD16/32 (5 µg/mL; BioXCell), followed by staining with fluorochrome-conjugated Ab. Fluorochrome-labeled anti-B220 (RA3-6B2), anti-CD3 (17A2), anti-CD4 (GK1.5), anti-CD11b (M1/70), anti-CD11c (HL3), anti-CD43 (S7), anti-CD44 (IM7), anti-CD45.1 (A20), anti-CD45.2 (104), anti-CD62L (MEL-14), anti-CD90.1 (OX-7), anti-CD90.2 (53-2.1), anti-CD103 (M290), anti-CD117 (2B8), anti-CCR7 (4B12), anti-Ly6C (AL-21), anti-Ly6G (IA8), anti-NK1.1 (PK136), anti-Siglec-F (E50-2440), and anti-TER-119 (TER-119), were from BD Biosciences. Fluorochrome-labeled anti-CD64 (X54-5/7.1), anti-CCR2 (SA203G11), anti-CX3CR1 (SA011F11), anti-Fc epsilon RI alpha (MAR-1), anti-MHC class II (M5/114.15.2), and anti-XCR1 (ZET) were from Biolegend. Fluorochrome-labeled anti-CD49b (DX5), anti-CD115 (AFS98), anti-CD127 (A7R34), anti-mertK (DS5MMER) were from eBioscience. Dead cell exclusion was performed using 7-AAD (Calbiochem). For intracellular cytokine staining of T cells, cell suspensions were stimulated with PMA (20 ng/mL) plus Calcimycin (1 µg/mL) in the presence of BD GolgiPlug for 4 h. Restimulated cells were surface stained, fixed and permeabilized with BD Cytotfix/Cytoperm Plus Kit and, stained with antibodies against IL-13 (13A; eBiosciences), IL-5 (TRFK5; BioLegend), IFN γ (XMG1.2; BD Biosciences), and IL-2 (JES6; BD Biosciences). For cytokine staining of DCs, cell suspensions were surface stained, fixed, permeabilized, and stained with anti-IL-12 (C15.6; BD-Biosciences). For TNF α , IL-1 β and GM-CSF staining, lung cell suspensions or sorted cells were incubated in the presence of BD GolgiPlug for 4-6 h, fixed, permeabilized, and stained with anti-TNF α (MP6-XT22; BD-Biosciences), anti-IL-1 β (NJTEN3; eBioscience), and anti-GM-CSF (MP1-22 $\times 10^9$; eBioscience). T-bet intracellular staining was performed using the Mouse regulatory T cell staining kit (eBioscience) and Abs against T-bet (4B10; biolegend), Flow cytometry was performed on Attune NxT and FACSCanto II (BD-Biosciences) instruments.

Cell purifications, sorting, cell transfers and *in vitro* cultures—CD4⁺ T cells were isolated by MACs (Miltenyi Biotec) from the spleens of naïve 4get.OTII TCR-transgenic mice. CD11c⁺ cells were isolated by MACs (CD11c MicroBeads UltraPure) from pooled mLN of day 3 sensitized mice. CD115⁺ monocytes were isolated by MACs from BM of naïve B6 mice. All cell preparations were more than 95% pure. Sensitization greatly induces migration of mDC2s and purification of CD11c⁺ cells from the mLNs of sensitized mice resulted in more than 80–90% enrichment of CD11c⁺MHC^{hi} mDC2s. For some experiments, BM monocytes were sorted, after staining with fluorochrome-conjugated CD11b, Ly6C, CD115, Ly6G and CCR2. All sorting experiments were performed using a FACSAria (BD Biosciences) sorter in the University of Alabama at Birmingham Flow Cytometry core. Sorted cells were more than 98% pure as determined by flow cytometry. Equivalent numbers (25×10^3) of naïve OTII cells were transferred (i.v.) into naïve congenic recipients. For i.n. transference of mDCs, purified monocytes (0.2×10^6 /ml) were cultured in complete medium containing GM-CSF (5 ng/mL; PeproTech) for 24 h. Equivalent numbers ($3-5 \times 10^5$) of cells were transferred (i.n.) into recipients daily for 3 days. For *in vitro* cultures, 4get.OTII cells were labeled for 10 min at 37°C with CellTrace CTV (Molecular Probes, ThermoFischer Scientific). 2×10^4 DCs and 1×10^5 CTV-labeled 4get.OTII cells were cultured in 200 μ L of complete medium in round-bottomed 96-well plates for 96 h at 37°C. Complete medium included RPMI 1640 supplemented with sodium pyruvate, HEPES, non-essential amino acids, penicillin, streptomycin, 2-mercaptoethanol and 10% heat-inactivated FBS from Fisher Scientific.

BAL collection and measurement of cytokines—BAL was collected using 0.5-1 mL sterilized PBS per mouse. The BAL fluids were centrifuged at $5,000 \times g$ for 10 min and the supernatants were frozen at -80°C . GM-CSF measurement was performed using GM-CSF Mouse Uncoated ELISA Kit (50-112-8722; Invitrogen). TNF α measurement was performed using TNF α Mouse ELISA Kit (MTA00B; R&D Systems).

HDM-specific IgE antibody measurement—96-well plates (Corning Clear Polystyrene 96-Well Microplates) were coated overnight with HDM extracts at 200 $\mu\text{g}/\text{mL}$ in 0.05 M Na₂CO₃ pH 9.6. Coated plates were then blocked for 1 h with 1% BSA in PBS. Serum from mice was collected and serially diluted (threefold) in PBS with 10 mg/mL BSA and 0.1% Tween 20 before incubation on coated plates. After washing, bound antibody was detected with HRP-conjugated goat Anti-Mouse IgE (1:2,000, 1110-05; Southern Biotech) and quantified by spectrophotometry at 405 nm (OD).

RNA-sequencing (RNA-seq)

Primary analysis: The quality of raw sequence fastq-formatted files was assessed using fastQC (<http://www.bioinformatics.babraham.ac.uk/projects/fastqc>). Sequences were trimmed using Trim Galore using phred33 scores (version 0.4.4, http://www.bioinformatics.babraham.ac.uk/projects/trim_galore), the paired setting and the nextera adapter option. Trimmed sequences were aligned with STAR aligner (Dobin et al., 2013) (version 2.5.2a) using mouse mm10 (UCSC) genome (https://support.illumina.com/sequencing/sequencing_software/igenome.html) and ENCODE options (outputFilterMultimapNmax = 20, alignSJoverhangMin = 8, alignSJD

BoverhangMin = 1, outFilterMismatchNmax = 999, alignIntronMin = 20, alignIntronMax = 1000000, alignMatesGapMax = 1000000). The STAR genome was constructed using the mm10 annotation file and sjdbOverhang = 100 as recommended in the documentation. Aligned reads were counted with HTseq-count (version 0.6.1p1) (Anders et al., 2015) set for un-stranded and using the mm10 genes.gtf annotation file.

Downstream analysis: The R package edgeR (Robinson et al., 2010) was used to assess differential expression between pairs of groups and to generate gene-by-sample matrices (for both RPKM and CPM). Because Ctrl and GM-CSF monocytes were derived from the same mouse per replicate, we then used a paired model. Volcano plot was performed using custom Matlab (The Mathworks Inc., Natick MA, USA) scripts. Comparison of our data to other published data sets was accomplished using Gene Set Enrichment Analysis (GSEA) (Subramanian et al., 2005).

QUANTIFICATION AND STATISTICAL ANALYSIS

All plots and histograms were plotted in FlowJo v.9 software (Treestar). GraphPad Prism (Version 9) was used for data analysis. The statistical significance of differences in mean values was determined using two-tailed Student's t test or one-way/two-way ANOVA with post-hoc Turkey's multiple comparison test. P values of less than 0.05 were considered statistically significant. * $P < 0.05$ ** $P < 0.01$ *** $P < 0.001$ **** $P < 0.0001$.

Supplementary Material

Refer to Web version on PubMed Central for supplementary material.

ACKNOWLEDGMENTS

We thank Becca Burnham, Uma Mudunuru, and Thomas S. Simpler for animal husbandry. The work was supported by UAB and NIH grants 2R01AI116584 to B. L. and R01AI150664 to A.B.T.

REFERENCES

- Anders S, Pyl PT, and Huber W (2015). HTSeq—a Python framework to work with high-throughput sequencing data. *Bioinformatics* 31, 166–169. 10.1093/bioinformatics/btu638. [PubMed: 25260700]
- Asokanathan N, Graham PT, Stewart DJ, Bakker AJ, Eidne KA, Thompson PJ, and Stewart GA (2002). House dust mite allergens induce proinflammatory cytokines from respiratory epithelial cells: the cysteine protease allergen, Der p 1, activates protease-activated receptor (PAR)-2 and inactivates PAR-1. *J. Immunol* 169, 4572–4578. 10.4049/jimmunol.169.8.4572. [PubMed: 12370395]
- Auffray C, Fogg D, Garfa M, Elain G, Join-Lambert O, Kayal S, Sarnacki S, Cumano A, Lauvau G, and Geissmann F (2007). Monitoring of blood vessels and tissues by a population of monocytes with patrolling behavior. *Science* 317, 666–670. 10.1126/science.1142883. [PubMed: 17673663]
- Bachus H, Kaur K, Papillion AM, Marquez-Lago TT, Yu Z, Ballesteros-Tato A, Matalon S, and Leon B (2019). Impaired tumor-necrosis-factor-alpha-driven dendritic cell activation limits lipopolysaccharide-induced protection from allergic inflammation in infants. *Immunity* 50, 225–240.e4. 10.1016/j.immuni.2018.11.012. [PubMed: 30635238]
- Ballesteros-Tato A, Randall TD, Lund FE, Spolski R, Leonard WJ, and Leon B (2016). T follicular helper cell plasticity shapes pathogenic T helper 2 cell-mediated immunity to inhaled house dust mite. *Immunity* 44, 259–273. 10.1016/j.immuni.2015.11.017. [PubMed: 26825674]

- Bhat RK, Page K, Tan A, and Hershenson MB (2003). German cockroach extract increases bronchial epithelial cell interleukin-8 expression. *Clin. Exp. Allergy* 33, 35–42. 10.1046/j.1365-2222.2002.01481.x. [PubMed: 12534547]
- Bolte G, Bischof W, Borte M, Lehmann I, Wichmann HE, Heinrich J, and Group LS (2003). Early endotoxin exposure and atopy development in infants: results of a birth cohort study. *Clin. Exp. Allergy* 33, 770–776. 10.1046/j.1365-2222.2003.01665.x. [PubMed: 12801311]
- Bortolatto J, Borducchi E, Rodriguez D, Keller AC, Faquim-Mauro E, Bortoluci KR, Mucida D, Gomes E, Christ A, Schnyder-Candrian S, et al. (2008). Toll-like receptor 4 agonists adsorbed to aluminium hydroxide adjuvant attenuate ovalbumin-specific allergic airway disease: role of MyD88 adaptor molecule and interleukin-12/interferon-gamma axis. *Clin. Exp. Allergy* 38, 1668–1679. 10.1111/j.1365-2222.2008.03036.x. [PubMed: 18631348]
- Braun-Fahrlander C, Gassner M, Grize L, Neu U, Sennhauser FH, Varonier HS, Vuille JC, and Wuthrich B (1999). Prevalence of hay fever and allergic sensitization in farmer's children and their peers living in the same rural community. SCARPOL team. Swiss Study on Childhood Allergy and Respiratory Symptoms with Respect to Air Pollution. *Clin. Exp. Allergy* 29, 28–34. 10.1046/j.1365-2222.1999.00479.x. [PubMed: 10051699]
- Braun-Fahrlander C, Riedler J, Herz U, Eder W, Waser M, Grize L, Maisch S, Carr D, Gerlach F, Bufe A, et al. (2002). Environmental exposure to endotoxin and its relation to asthma in school-age children. *N. Engl. J. Med* 347, 869–877. 10.1056/NEJMoa020057. [PubMed: 12239255]
- Carlin LM, Stamatiades EG, Auffray C, Hanna RN, Glover L, Vizcay-Barrena G, Hedrick CC, Cook HT, Diebold S, and Geissmann F (2013). Nr4a1-dependent Ly6C(low) monocytes monitor endothelial cells and orchestrate their disposal. *Cell* 153, 362–375. 10.1016/j.cell.2013.03.010. [PubMed: 23582326]
- Cayrol C, Duval A, Schmitt P, Roga S, Camus M, Stella A, Burlet-Schiltz O, Gonzalez-de-Peredo A, and Girard JP (2018). Environmental allergens induce allergic inflammation through proteolytic maturation of IL-33. *Nat. Immunol* 19, 375–385. 10.1038/s41590-018-0067-5. [PubMed: 29556000]
- Celedon JC, Milton DK, Ramsey CD, Litonjua AA, Ryan L, Platts-Mills TA, and Gold DR (2007). Exposure to dust mite allergen and endotoxin in early life and asthma and atopy in childhood. *J. Allergy Clin. Immunol* 120, 144–149. 10.1016/j.jaci.2007.03.037. [PubMed: 17507083]
- Delayre-Orthez C, de Blay F, Frossard N, and Pons F (2004). Dose-dependent effects of endotoxins on allergen sensitization and challenge in the mouse. *Clin. Exp. Allergy* 34, 1789–1795. 10.1111/j.1365-2222.2004.02082.x. [PubMed: 15544606]
- Dharmage SC, Perret JL, and Custovic A (2019). Epidemiology of asthma in children and adults. *Front Pediatr.* 7, 246. 10.3389/fped.2019.00246. [PubMed: 31275909]
- Dobin A, Davis CA, Schlesinger F, Drenkow J, Zaleski C, Jha S, Batut P, Chaisson M, and Gingeras TR (2013). STAR: ultrafast universal RNA-seq aligner. *Bioinformatics* 29, 15–21. 10.1093/bioinformatics/bts635. [PubMed: 23104886]
- Eder W, Klimecki W, Yu L, von Mutius E, Riedler J, Braun-Fahrlander C, Nowak D, and Martinez FD; Allergy and Endotoxin Alex Study Team (2005). Opposite effects of CD 14/–260 on serum IgE levels in children raised in different environments. *J. Allergy Clin. Immunol* 116, 601–607. 10.1016/j.jaci.2005.05.003. [PubMed: 16159630]
- Eder W, Klimecki W, Yu L, von Mutius E, Riedler J, Braun-Fahrlander C, Nowak D, Martinez FD, and Team AS (2004). Toll-like receptor 2 as a major gene for asthma in children of European farmers. *J. Allergy Clin. Immunol* 113, 482–488. 10.1016/j.jaci.2003.12.374. [PubMed: 15007351]
- Eder W, and von Mutius E (2004). Hygiene hypothesis and endotoxin: what is the evidence? *Curr. Opin. Allergy Clin. Immunol* 4, 113–117. 10.1097/00130832-200404000-00008. [PubMed: 15021064]
- Eisenbarth SC, Piggott DA, Huleatt JW, Visintin I, Herrick CA, and Bottomly K (2002). Lipopolysaccharide-enhanced, toll-like receptor 4-dependent T helper cell type 2 responses to inhaled antigen. *J. Exp. Med* 196, 1645–1651. 10.1084/jem.20021340. [PubMed: 12486107]
- Gamrekelashvili J, Giagnorio R, Jussofie J, Soehnlein O, Duchene J, Briseno CG, Ramasamy SK, Krishnasamy K, Limbourg A, Kapanadze T, et al. (2016). Regulation of monocyte cell fate by blood vessels mediated by Notch signalling. *Nat. Commun* 7, 12597. 10.1038/ncomms12597. [PubMed: 27576369]

- Gandhi VD, and Vliagoftis H (2015). Airway epithelium interactions with aeroallergens: role of secreted cytokines and chemokines in innate immunity. *Front Immunol.* 6, 147. 10.3389/fimmu.2015.00147. [PubMed: 25883597]
- Gehring U, Bischof W, Fahlbusch B, Wichmann HE, and Heinrich J (2002). House dust endotoxin and allergic sensitization in children. *Am. J. Respir. Crit. Care Med* 166, 939–944. 10.1164/rccm.200203-256OC. [PubMed: 12359650]
- Geissmann F, Jung S, and Littman DR (2003). Blood monocytes consist of two principal subsets with distinct migratory properties. *Immunity* 19, 71–82. 10.1016/s1074-7613(03)00174-2. [PubMed: 12871640]
- Gereda JE, Klinnert MD, Price MR, Leung DY, and Liu AH (2001). Metropolitan home living conditions associated with indoor endotoxin levels. *J. Allergy Clin. Immunol* 107, 790–796. 10.1067/mai.2001.115245. [PubMed: 11344344]
- Gereda JE, Leung DY, Thatayatikom A, Streib JE, Price MR, Klinnert MD, and Liu AH (2000). Relation between house-dust endotoxin exposure, type 1 T-cell development, and allergen sensitisation in infants at high risk of asthma. *Lancet* 355, 1680–1683. 10.1016/s0140-6736(00)02239-x. [PubMed: 10905243]
- Hammad H, Chieppa M, Perros F, Willart MA, Germain RN, and Lambrecht BN (2009). House dust mite allergen induces asthma via Toll-like receptor 4 triggering of airway structural cells. *Nat. Med* 15, 410–416. 10.1038/nm.1946. [PubMed: 19330007]
- Kim YK, Oh SY, Jeon SG, Park HW, Lee SY, Chun EY, Bang B, Lee HS, Oh MH, Kim YS, et al. (2007). Airway exposure levels of lipopolysaccharide determine type 1 versus type 2 experimental asthma. *J. Immunol* 178, 5375–5382. 10.4049/jimmunol.178.8.5375. [PubMed: 17404323]
- Leomicronn B (2017). T cells in allergic asthma: key players beyond the Th2 pathway. *Curr. Allergy Asthma Rep* 17, 43. 10.1007/s11882-017-0714-1. [PubMed: 28555329]
- Leon B, and Ballesteros-Tato A (2021). Modulating Th2 cell immunity for the treatment of asthma. *Front Immunol.* 12, 637948. 10.3389/fimmu.2021.637948. [PubMed: 33643321]
- Leon B, Ballesteros-Tato A, Browning JL, Dunn R, Randall TD, and Lund FE (2012). Regulation of T(H)2 development by CXCR5+ dendritic cells and lymphotoxin-expressing B cells. *Nat. Immunol* 13, 681–690. 10.1038/ni.2309. [PubMed: 22634865]
- Liu AH, and Leung DY (2006). Renaissance of the hygiene hypothesis. *J. Allergy Clin. Immunol* 117, 1063–1066. 10.1016/j.jaci.2006.03.027. [PubMed: 16675333]
- Llop-Guevara A, Chu DK, Walker TD, Goncharova S, Fattouh R, Silver JS, Moore CL, Xie JL, O’Byrne PM, Coyle AJ, et al. (2014). A GM-CSF/IL-33 pathway facilitates allergic airway responses to sub-threshold house dust mite exposure. *PLoS One* 9, e88714. 10.1371/journal.pone.0088714. [PubMed: 24551140]
- McAlees JW, Whitehead GS, Harley IT, Cappelletti M, Rewerts CL, Holdcroft AM, Divanovic S, Wills-Karp M, Finkelman FD, Karp CL, and Cook DN (2015). Distinct Tlr4-expressing cell compartments control neutrophilic and eosinophilic airway inflammation. *Mucosal Immunol.* 8, 863–873. 10.1038/mi.2014.117. [PubMed: 25465099]
- Medvedev AE (2013). Toll-like receptor polymorphisms, inflammatory and infectious diseases, allergies, and cancer. *J. Interferon Cytokine Res* 33, 467–484. 10.1089/jir.2012.0140. [PubMed: 23675778]
- Misharin AV, Cuda CM, Saber R, Turner JD, Gierut AK, Haines GK 3rd, Berdnikovs S, Filer A, Clark AR, Buckley CD, et al. (2014). Nonclassical Ly6C(–) monocytes drive the development of inflammatory arthritis in mice. *Cell Rep.* 9, 591–604. 10.1016/j.celrep.2014.09.032. [PubMed: 25373902]
- Nakano H, Burgents JE, Nakano K, Whitehead GS, Cheong C, Bortner CD, and Cook DN (2013). Migratory properties of pulmonary dendritic cells are determined by their developmental lineage. *Mucosal. Immunol* 6, 678–691. 10.1038/mi.2012.106. [PubMed: 23168837]
- Narasimhan PB, Marcovecchio P, Hamers AAJ, and Hedrick CC (2019). Nonclassical monocytes in health and disease. *Annu. Rev. Immunol* 37, 439–456. 10.1146/annurev-immunol-042617-053119. [PubMed: 31026415]

- Nathan AT, Peterson EA, Chakir J, and Wills-Karp M (2009). Innate immune responses of airway epithelium to house dust mite are mediated through beta-glucan-dependent pathways. *J. Allergy Clin. Immunol* 123, 612–618. 10.1016/j.jaci.2008.12.006. [PubMed: 19178937]
- Olingy CE, San Emeterio CL, Ogle ME, Krieger JR, Bruce AC, Pfau DD, Jordan BT, Peirce SM, and Botchwey EA (2017). Non-classical monocytes are biased progenitors of wound healing macrophages during soft tissue injury. *Sci. Rep* 7, 447. 10.1038/s41598-017-00477-1. [PubMed: 28348370]
- Page K, Ledford JR, Zhou P, Dienger K, and Wills-Karp M (2010). Mucosal sensitization to German cockroach involves protease-activated receptor-2. *Respir. Res* 11, 62. 10.1186/1465-9921-11-62. [PubMed: 20497568]
- Perner C, Flayer CH, Zhu X, Aderhold PA, Dewan ZNA, Voisin T, Camire RB, Chow OA, Chiu IM, and Sokol CL (2020). Substance P release by sensory neurons triggers dendritic cell migration and initiates the type-2 immune response to allergens. *Immunity* 53, 1063–1077.e7. 10.1016/j.immuni.2020.10.001. [PubMed: 33098765]
- Plantinga M, Guillems M, Vanheerswyngheles M, Deswarte K, Branco-Madeira F, Toussaint W, Vanhoutte L, Neyt K, Killeen N, Malissen B, et al. (2013). Conventional and monocyte-derived CD11b(+) dendritic cells initiate and maintain T helper 2 cell-mediated immunity to house dust mite allergen. *Immunity* 38, 322–335. 10.1016/j.immuni.2012.10.016. [PubMed: 23352232]
- Polley DJ, Mihara K, Ramachandran R, Vliagoftis H, Renaux B, Saifeddine M, Daines MO, Boitano S, and Hollenberg MD (2017). Cockroach allergen serine proteinases: isolation, sequencing and signalling via proteinase-activated receptor-2. *Clin. Exp. Allergy* 47, 946–960. 10.1111/cea.12921.. [PubMed: 28317204]
- Quintar A, McArdle S, Wolf D, Marki A, Ehinger E, Vassallo M, Miller J, Mikulski Z, Ley K, and Buscher K (2017). Endothelial protective monocyte patrolling in large arteries intensified by Western diet and atherosclerosis. *Circ. Res* 120, 1789–1799. 10.1161/CIRCRESAHA.117.310739. [PubMed: 28302649]
- Radermecker C, Sabatel C, Vanwinge C, Ruscitti C, Marechal P, Perin F, Schyns J, Rocks N, Toussaint M, Cataldo D, et al. (2019). Locally instructed CXCR4(hi) neutrophils trigger environment-driven allergic asthma through the release of neutrophil extracellular traps. *Nat. Immunol* 20, 1444–1455. 10.1038/s41590-019-0496-9. [PubMed: 31591573]
- Radon K (2006). The two sides of the "endotoxin coin". *Occup. Environ. Med* 63, 73–78. 10.1136/oem.2004.017616. [PubMed: 16361410]
- Reithofer M, and Jahn-Schmid B (2017). Allergens with protease activity from house dust mites. *Int. J. Mol. Sci* 18. 10.3390/ijms18071368.
- Robinson MD, McCarthy DJ, and Smyth GK (2010). edgeR: a Bioconductor package for differential expression analysis of digital gene expression data. *Bioinformatics* 26, 139–140. 10.1093/bioinformatics/btp616. [PubMed: 19910308]
- Ryu JH, Yoo JY, Kim MJ, Hwang SG, Ahn KC, Ryu JC, Choi MK, Joo JH, Kim CH, Lee SN, et al. (2013). Distinct TLR-mediated pathways regulate house dust mite-induced allergic disease in the upper and lower airways. *J. Allergy Clin. Immunol* 131, 549–561. 10.1016/j.jaci.2012.07.050. [PubMed: 23036747]
- Serhan N, Basso L, Sibilano R, Petitfils C, Meixiong J, Bonnart C, Reber LL, Marichal T, Starkl P, Cenac N, et al. (2019). House dust mites activate nociceptor-mast cell clusters to drive type 2 skin inflammation. *Nat. Immunol* 20, 1435–1443. 10.1038/s41590-019-0493-z. [PubMed: 31591569]
- Sheih A, Parks WC, and Ziegler SF (2017). GM-CSF produced by the airway epithelium is required for sensitization to cockroach allergen. *Mucosal. Immunol* 10, 705–715. 10.1038/mi.2016.90. [PubMed: 27731325]
- Stampfli MR, Wiley RE, Neigh GS, Gajewska BU, Lei XF, Snider DP, Xing Z, and Jordana M (1998). GM-CSF transgene expression in the airway allows aerosolized ovalbumin to induce allergic sensitization in mice. *J. Clin. Invest* 102, 1704–1714. 10.1172/JCI14160. [PubMed: 9802884]
- Stein MM, Hrusch CL, Gozdz J, Igartua C, Pivniouk V, Murray SE, Ledford JG, Marques Dos Santos M, Anderson RL, Metwali N, et al. (2016). Innate immunity and asthma risk in Amish and Hutterite farm children. *N. Engl. J. Med* 375, 411–421.10.1056/NEJMoa1508749. [PubMed: 27518660]

- Subramanian A, Tamayo P, Mootha VK, Mukherjee S, Ebert BL, Gillette MA, Paulovich A, Pomeroy SL, Golub TR, Lander ES, and Mesirov JP (2005). Gene set enrichment analysis: a knowledge-based approach for interpreting genome-wide expression profiles. *Proc. Natl. Acad. Sci. U S A* 102, 15545–15550. 10.1073/pnas.0506580102. [PubMed: 16199517]
- Sunderkotter C, Nikolic T, Dillon MJ, Van Rooijen N, Stehling M, Drevets DA, and Leenen PJ (2004). Subpopulations of mouse blood monocytes differ in maturation stage and inflammatory response. *J. Immunol* 172, 4410–4417. 10.4049/jimmunol.172.7.4410. [PubMed: 15034056]
- Tan AM, Chen HC, Pochard P, Eisenbarth SC, Herrick CA, and Bottomly HK (2010). TLR4 signaling in stromal cells is critical for the initiation of allergic Th2 responses to inhaled antigen. *J. Immunol* 184, 3535–3544. 10.4049/jimmunol.0900340. [PubMed: 20194715]
- Tsakamoto H, Fukudome K, Takao S, Tsuneyoshi N, Ohta S, Nagai Y, Ihara H, Miyake K, Ikeda Y, and Kimoto M (2013). Reduced surface expression of TLR4 by a V254I point mutation accounts for the low lipopolysaccharide responder phenotype of BALB/c B cells. *J. Immunol* 190, 195–204. 10.4049/jimmunol.1201047. [PubMed: 23203928]
- Varol C, Landsman L, Fogg DK, Greenshtein L, Gildor B, Margalit R, Kalchenko V, Geissmann F, and Jung S (2007). Monocytes give rise to mucosal, but not splenic, conventional dendritic cells. *J. Exp. Med* 204, 171–180. 10.1084/jem.20061011. [PubMed: 17190836]
- Vercelli D (2008). Discovering susceptibility genes for asthma and allergy. *Nat. Rev. Immunol* 8, 169–182. 10.1038/nri2257. [PubMed: 18301422]
- von Mutius E, Braun-Fahrlander C, Schierl R, Riedler J, Ehlermann S, Maisch S, Waser M, and Nowak D (2000). Exposure to endotoxin or other bacterial components might protect against the development of atopy. *Clin. Exp. Allergy* 30, 1230–1234. 10.1046/j.1365-2222.2000.00959.x. [PubMed: 10971468]
- Wilson RH, Maruoka S, Whitehead GS, Foley JF, Flake GP, Sever ML, Zeldin DC, Kraft M, Garantziotis S, Nakano H, and Cook DN (2012). The Toll-like receptor 5 ligand flagellin promotes asthma by priming allergic responses to indoor allergens. *Nat. Med* 18, 1705–1710. 10.1038/nm.2920. [PubMed: 23064463]
- Yona S, Kim KW, Wolf Y, Mildner A, Varol D, Breker M, Strauss-Ayali D, Viukov S, Guillemins M, Misharin A, et al. (2013). Fate mapping reveals origins and dynamics of monocytes and tissue macrophages under homeostasis. *Immunity* 38, 79–91. 10.1016/j.immuni.2012.12.001. [PubMed: 23273845]

Highlights

- LPS can promote or suppress Th2 cell sensitization depending on GM-CSF production
- GM-CSF is produced by Ly6C^{lo} monocytes in response to cysteine protease allergens
- GM-CSF induces differentiation of LPS-sensitive moDCs that instruct for Th2 suppression
- Without GM-CSF, Th2-dependent sensitization is favored due to the lack of moDCs

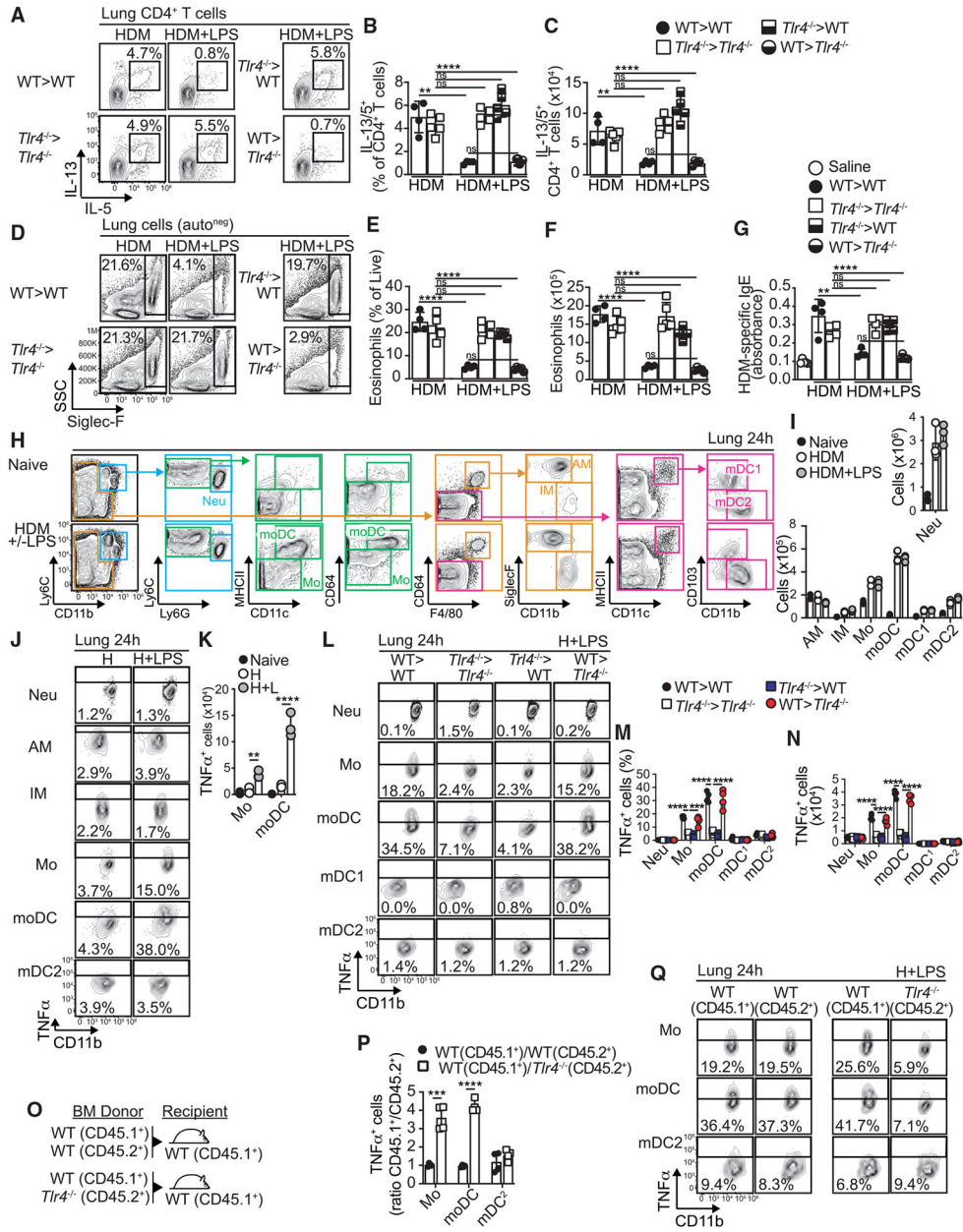


Figure 1. TLR4 sensing triggers monocyte and moDC activation upon HDM + LPS exposure (A–G) Chimeric mice were sensitized and challenged. Frequencies (A and B) and numbers (C) of IL-13⁺IL-5⁺ CD4⁺ T cells in the lungs. Frequencies (D and E) and numbers (F) of eosinophils in the lungs. HDM-specific IgE levels in serum (G). (H–K) Lungs from naive and HDM ± LPS-treated B6 mice were analyzed. Cell identification strategy (H), numbers of indicated cell populations (I) and frequencies (J), and numbers (K) of TNFα⁺ cell types. (L–N) Chimeric mice were treated with HDM + LPS. Frequencies (L and M) and numbers (N) of TNFα⁺ cell types in the lung. (O–Q) WT:WT and WT: *Tlr4*^{-/-} chimeras were generated (O). Frequencies (Q) and ratio (P) of TNFα⁺ WT and *Tlr4*^{-/-} cell types in the lung of HDM ± LPS-treated mice.

Data are representative of three independent experiments (mean \pm SD, n = 3–5, one-way ANOVA). *p < 0.05, **p < 0.01, ***p < 0.001, ****p < 0.0001. See Figures S1-S4.

Author Manuscript

Author Manuscript

Author Manuscript

Author Manuscript

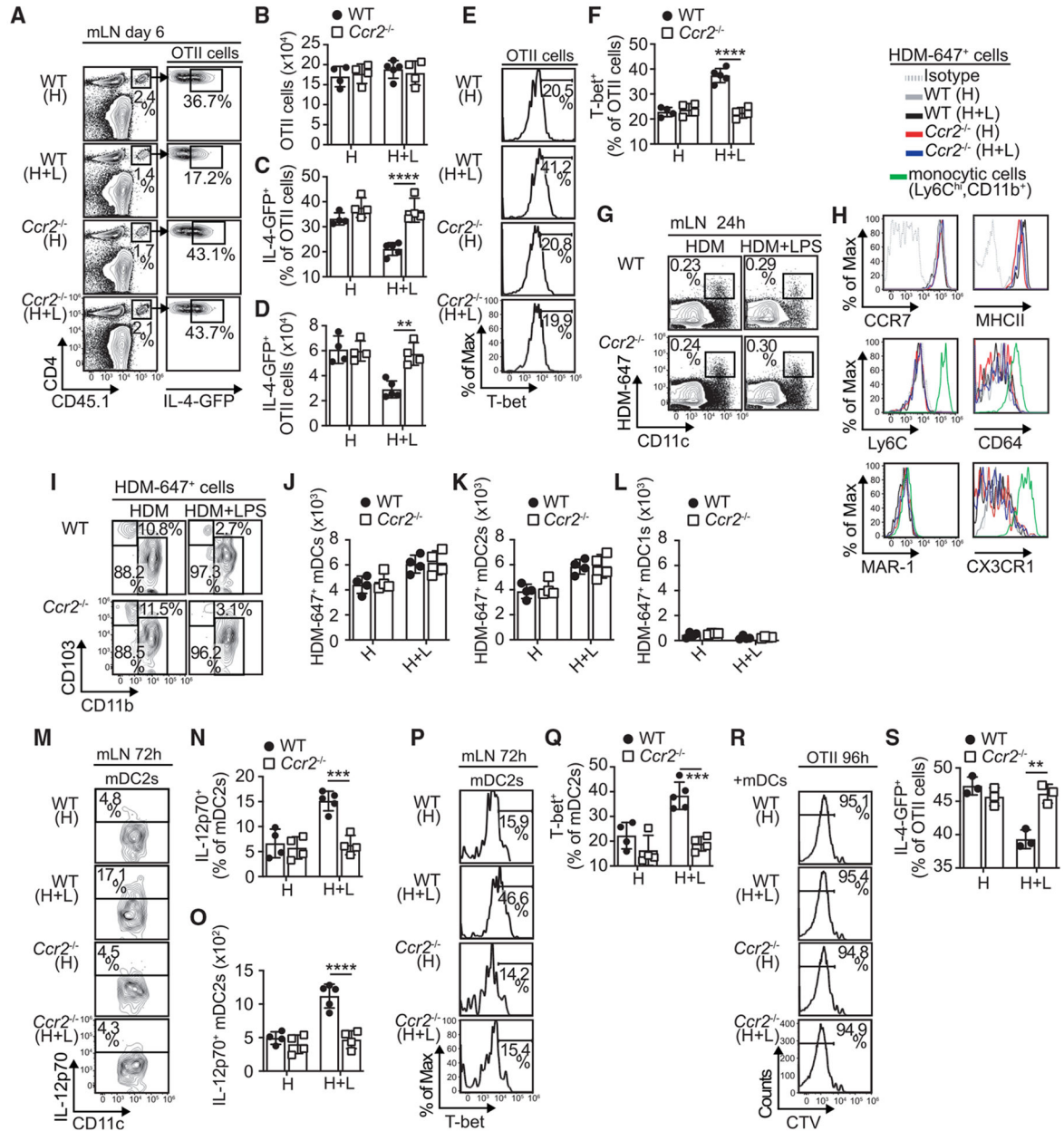


Figure 2. CCR2 is required for LPS-driven suppression of allergen-specific Th2 cell responses (A–F) Mice were transferred with OT-II.4get cells and sensitized. Frequencies (A, C, E, and F) and numbers (B and D) of total, IL-4-GFP⁺, and T-bet⁺ OT-II cells. (G–L) Mice were treated with Alexa Fluor 647-labeled HDM ± LPS. Frequencies of HDM⁺ cells (G) and expression of the indicated markers on HDM⁺ cells and monocytic cells (H). Frequencies (I) and numbers (J–L) of HDM⁺ mDCs (J), mDC2s (K), and mDC1s (L). (M–S) Frequencies (M and N) and numbers (O) of IL-12p70⁺ mDC2s, and frequencies (P and Q) of T-bet⁺ mDC2s in the mLN of HDM ± LPS-treated mice. (R and S) Day-3 mLN CD11c⁺ mDCs from sensitized mice were co-cultured for 4 days with CTV-labeled OT-II.4get cells. Frequencies of CTV⁺OTII cells (R), frequencies of IL-4-GFP expression in CTV⁺OTII cells (S). Values in triplicate.

Data are representative of three independent experiments (mean \pm SD, n = 4–5, two-way ANOVA). *p < 0.05, **p < 0.01, ***p < 0.001, ****p < 0.0001. See Figures S5-S7.

Author Manuscript

Author Manuscript

Author Manuscript

Author Manuscript

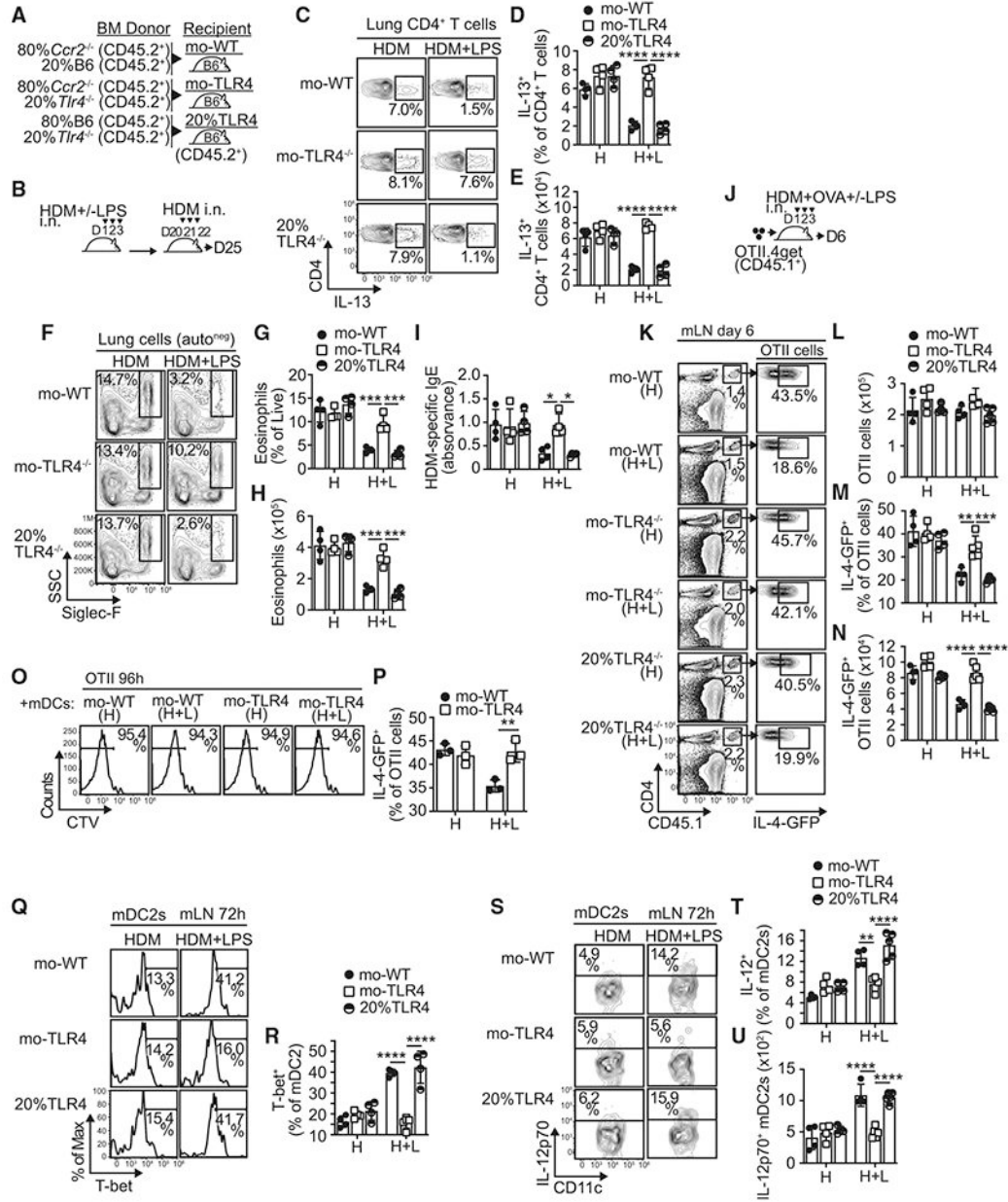


Figure 3. TLR4 expression in Ly6C^{hi} monocytic cells is required to license mDC2s to prevent allergen-specific Th2 cell responses upon LPS exposure

(A–I) Chimeric mice were generated (A) and sensitized and challenged (B). Frequencies (C and D) and numbers (E) of IL-13⁺ CD4⁺ T cells. Frequencies (F and G) and numbers (H) of eosinophils. HDM-specific IgE levels in serum (I).

(J–N) Mice were transferred with OT-II.4get cells and sensitized (J). Frequencies (K and M) and numbers (L and N) of total and IL-4-GFP⁺ OT-II cells.

(O–P) mLN CD11c⁺ mDCs from sensitized mice were co-cultured with naive OT-II.4get cells. Frequencies of CTV^{lo}OTII cells (O) and IL-4-GFP expression in CTV^{lo}OTII cells (P). Values in triplicate.

(Q–U) Frequencies of T-bet⁺ mDC2s (Q and R) and frequencies (S and T) and numbers (U) of IL-12p70⁺ mDC2s.

Data are representative of two independent experiments (mean ± SD, n = 4–5, two-way ANOVA). *p < 0.05, **p < 0.01, ***p < 0.001, ****p < 0.0001. See Figures S8 and S9.

Author Manuscript

Author Manuscript

Author Manuscript

Author Manuscript

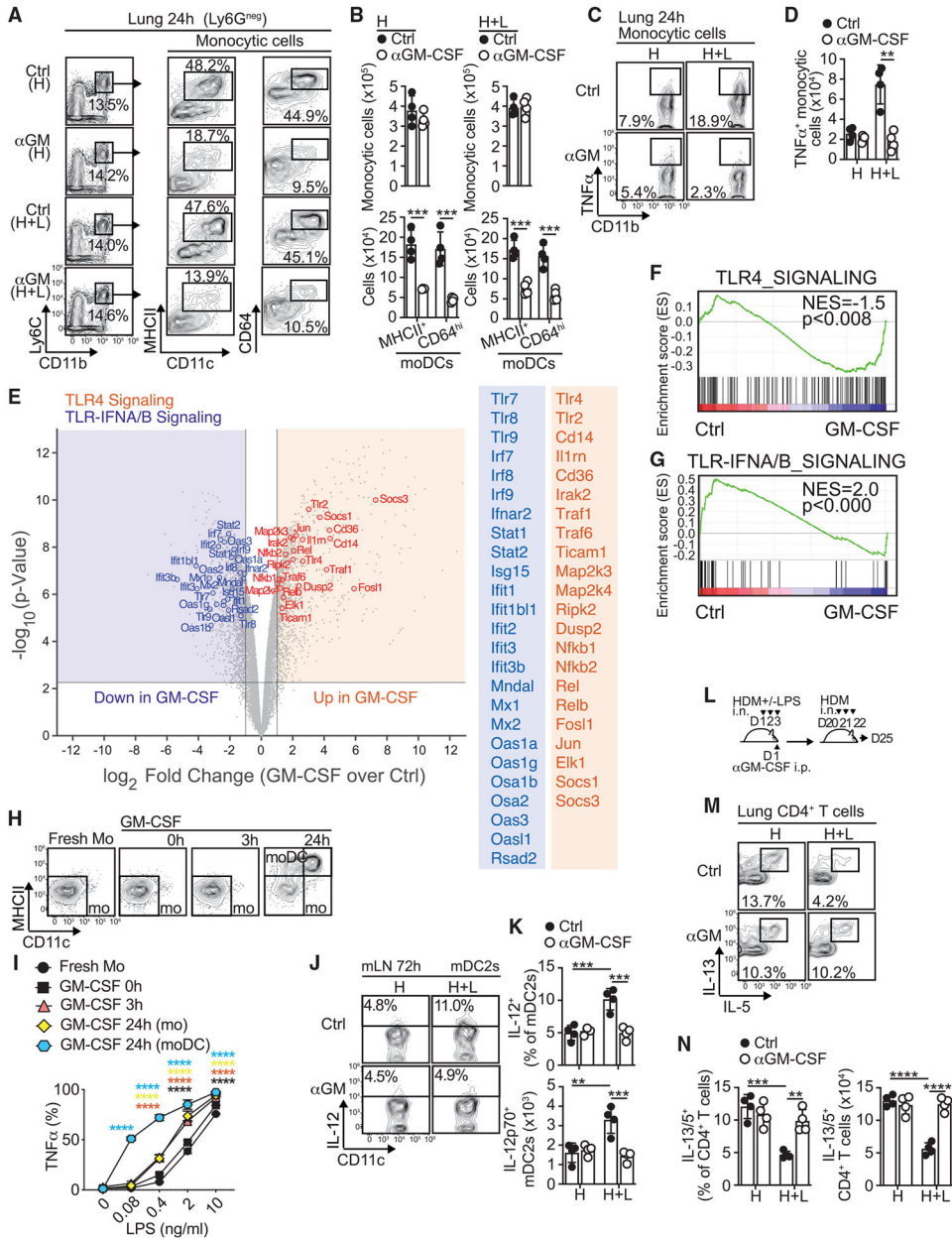


Figure 4. GM-CSF programs Ly6C^{hi} monocyte-derived cells to respond to low-dose LPS and contributes toward the prevention of Th2 cell development to HDM + LPS
 (A–D) B6 mice were sensitized and treated intraperitoneally (i.p.) with or without GM-CSF. Frequencies (A) and numbers (B) of Ly6C^{hi}CD11b⁺ monocytic cells and moDCs (CD11c⁺MHCII⁺ or CD11c⁺CD64^{hi} cells). Frequencies (C) and numbers (D) of TNFα⁺ monocytic cells.
 (E–G) Sorted Ly6C^{hi} monocytes were stimulated with or without GM-CSF for 3 h, and RNA-seq was performed (three replicates). Volcano plot highlighting DEG (E) from a total of 2,431 genes, with 1,177 upregulated and 1,254 downregulated (false discovery rate < 0.01, 2 fold change; see Table S1). Blue box displays gene members of PathCard TLR-IFNA/β signaling that are downregulated in GM-CSF versus Ctrl monocytes. Red box displays

gene members of PathCard TLR4 signaling that are upregulated in GM-CSF versus Ctrl monocytes. GSEA for the indicated gene signatures (F and G).

(H and I) Fresh and GM-CSF pre-treated monocytes were stimulated with LPS ± GM-CSF. Expression of CD11c, MHCII (H), and intracellular TNF α (I). Values in triplicate.

(J and K) Frequencies (J) and numbers (K) of IL-12p70⁺ mDC2s.

(L–N) B6 mice were treated as shown (L). Frequencies (M) and numbers (N) of IL-13⁺IL-5⁺ CD4⁺ T cells in the lungs.

Data are representative of three independent experiments (mean \pm SD, n = 4, two-way ANOVA). *p < 0.05, **p < 0.01, ***p < 0.001, ****p < 0.0001. See Figure S10 and Table S1.

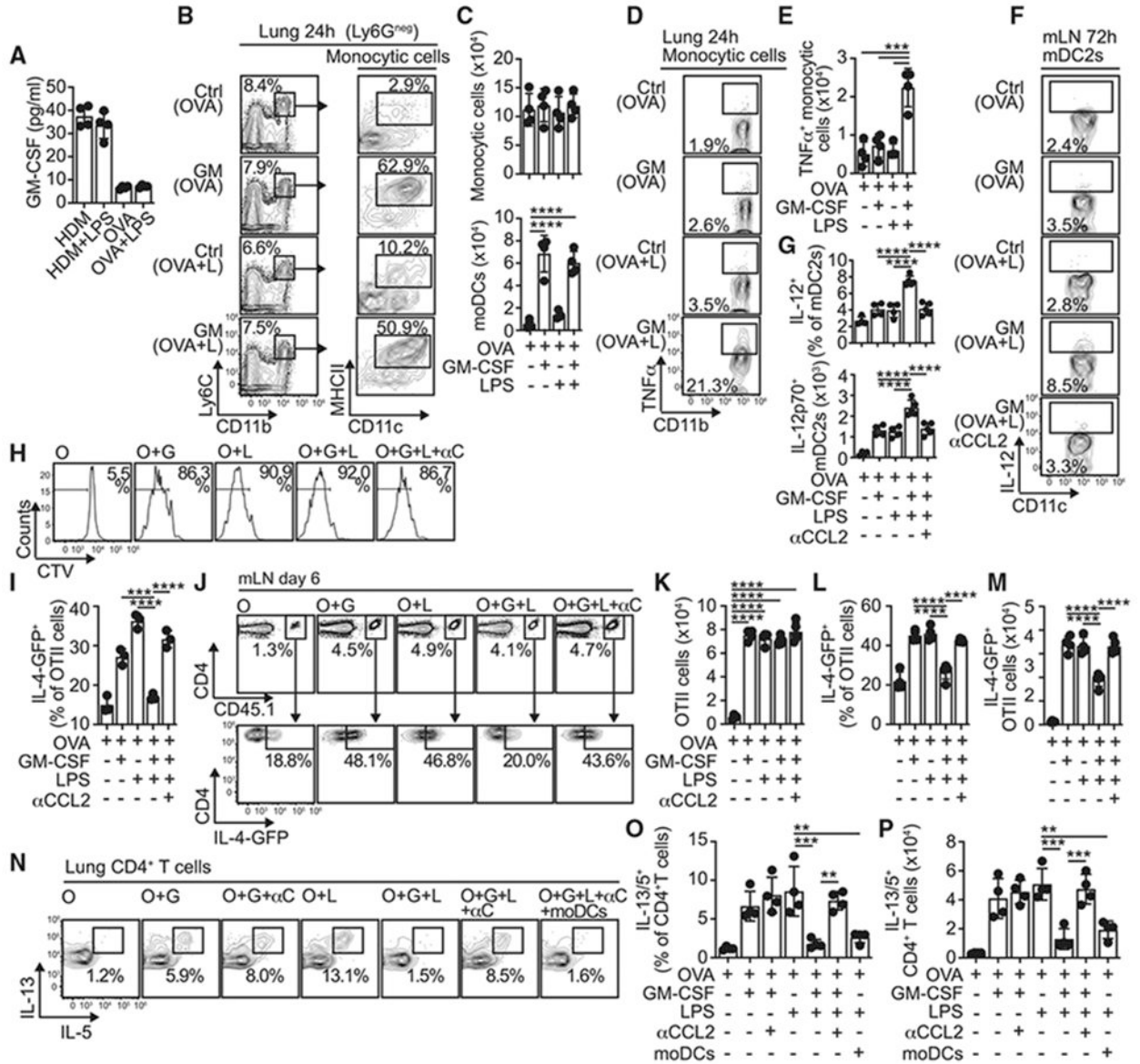


Figure 5. GM-CSF signaling in monocyte-derived cells licenses mDC2s to prevent allergen-specific Th2 cell responses upon low-dose LPS exposure

(A) GM-CSF in BAL on day 1 (B-I) B6 mice were sensitized and i.p. treated with or without CCL2.

(B and C) Frequencies (B) and numbers (C) of Ly6C^{hi}CD11b⁺ monocytic cells and CD11c⁺MHCII⁺ mDCs.

(D and E) Frequencies (D) and numbers (E) of TNFα⁺ monocytic cells.

(F and G) Frequencies (F) and numbers (G) of IL-12p70⁺ mDC2s.

(H and I) mLN mDCs were co-cultured with naive OT-II.4get cells. Frequencies of CTV^{lo}OTII cells (H) and IL-4-GFP expression in CTV^{lo}OTII cells (I). Values in triplicate.

(J–M) Mice were transferred with CD45.1⁺ OT-II.4get cells and sensitized. Frequencies (J and L) and numbers (K and M) of total and IL-4-GFP⁺ OT-II cells.

(N–P) Mice were sensitized and some received *in vitro* GM-CSF-generated moDCs (i.n.) or anti-CCL2 (i.p.). Mice were then challenged. Frequencies (N and O) and numbers (P) of IL-13⁺IL-5⁺ CD4⁺ T cells.

Data are representative of at least two independent experiments (mean ± SD, n = 4–5, one-way ANOVA). *p < 0.05, **p < 0.01, ***p < 0.001, ****p < 0.0001. See Figure S11.

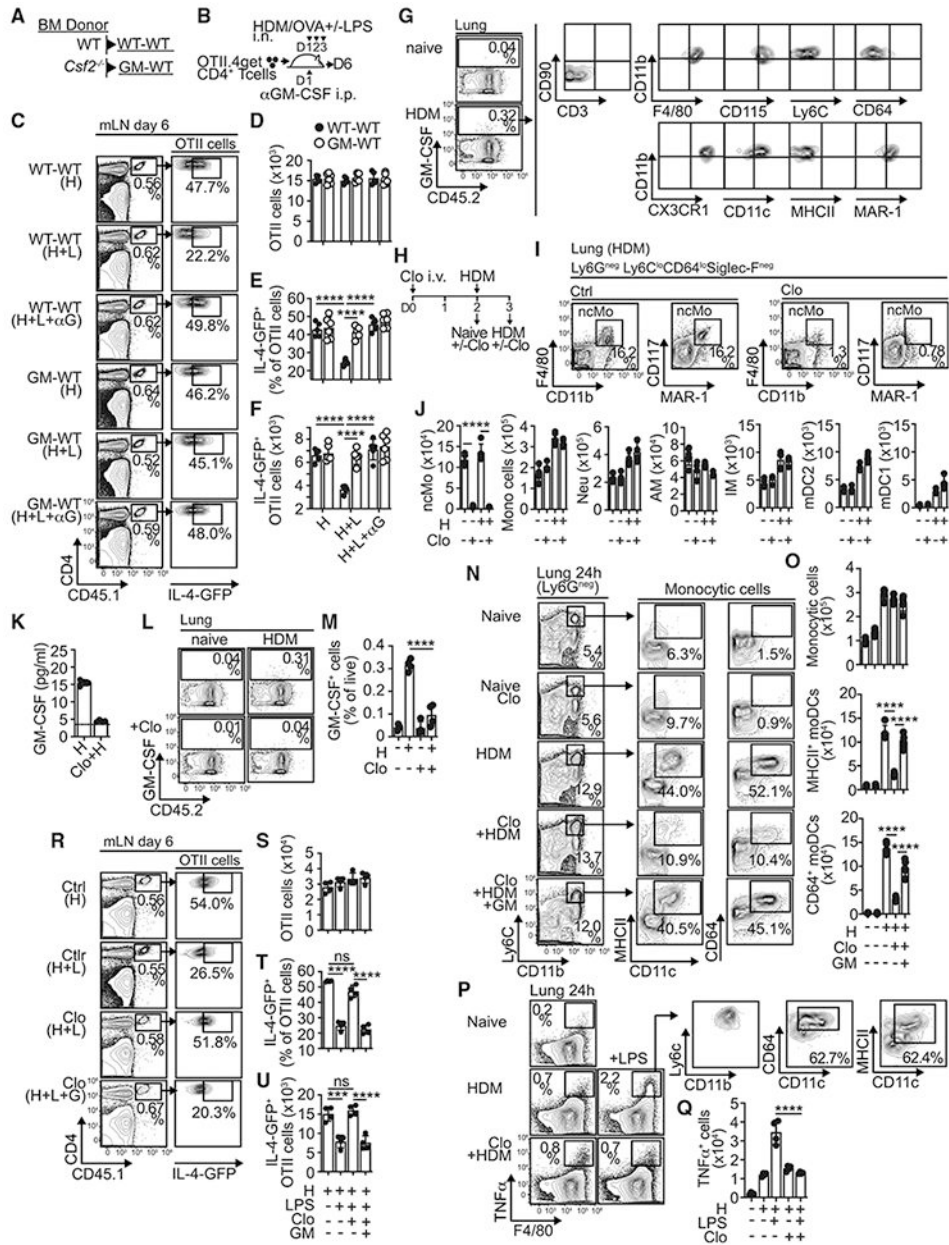


Figure 6. GM-CSF is produced by non-classical Ly6C^{lo} monocytes after HDM sensitization (A–F) Chimeric mice were generated (A) and treated as shown (B). Frequencies (C and E) and numbers (D and F) of total and IL-4-GFP⁺ OT-II cells. (G) CD45.2⁺>CD45.1⁺ chimeric mice were treated with or without HDM. Frequencies and phenotype of GM-CSF⁺ cells on day 1. (H–J) Mice were treated as shown (H) and lungs were analyzed on days 2 and 3. Frequencies of ncMo on day 3 (I). Numbers of indicated populations (J). (K) GM-CSF in BAL. (L and M) Frequencies of GM-CSF⁺ cells. (N–Q) Frequencies (N and P) and numbers (O and Q) of total Ly6C^{hi}CD11b⁺ monocytic cells, differentiated moDCs (CD11c⁺MHCII⁺ or CD11c⁺CD64^{hi} cells), and TNFα⁺ cells.

(R–U) Mice were transferred with CD45.1⁺ OT-II.4get cells and treated. Frequencies (R and T) and numbers (S and U) of total and IL-4-GFP⁺ OT-II cells.

Data are representative of at least two independent experiments (mean ± SD, n = 4–6, one-way ANOVA). *p < 0.05, **p < 0.01, ***p < 0.001, ****p < 0.0001. See Figures S12 and S13.

Author Manuscript

Author Manuscript

Author Manuscript

Author Manuscript

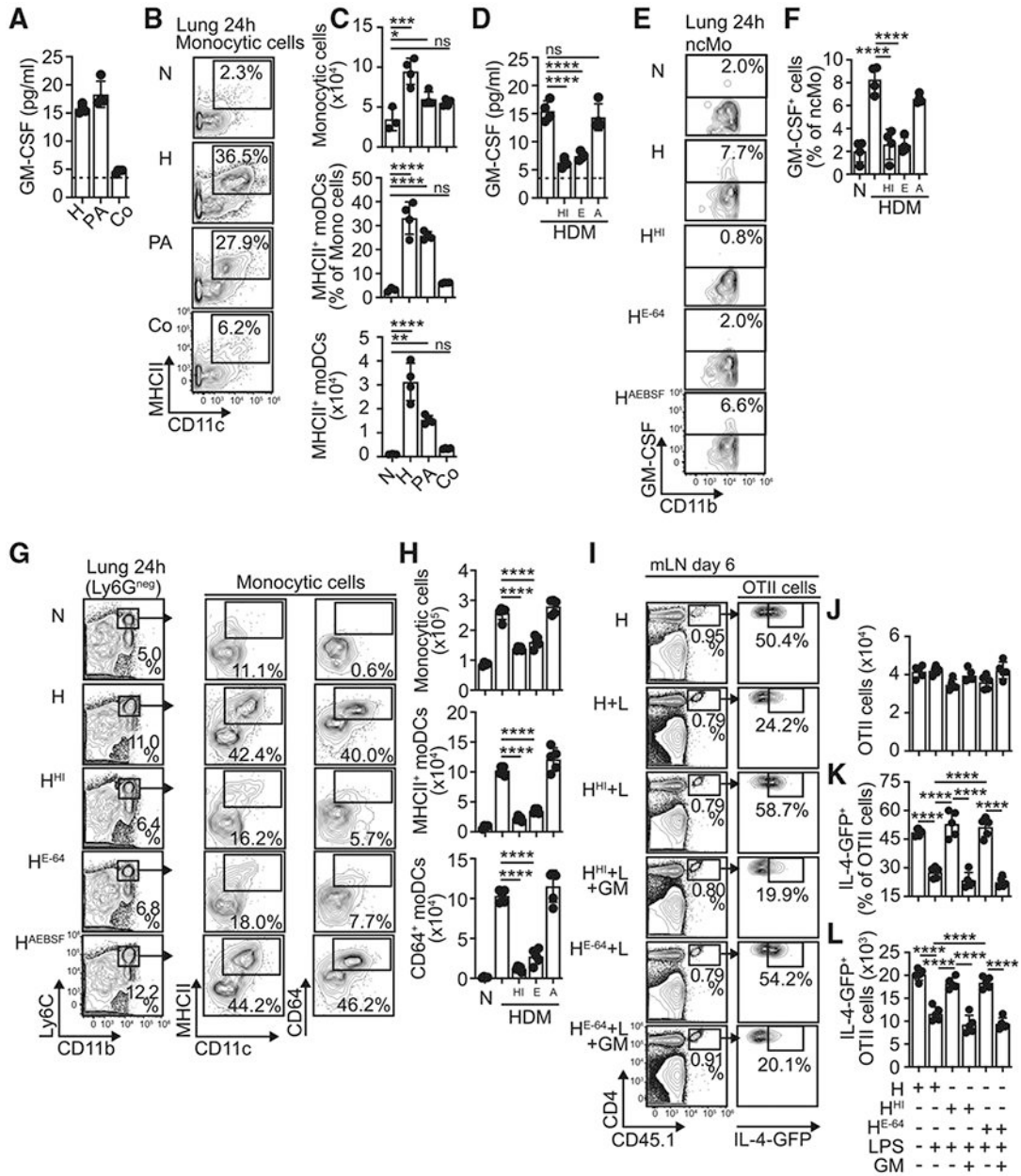


Figure 7. Cysteine protease activity in HDM is required for GM-CSF production and preventing Th2 cell responses

(A) GM-CSF in BAL of mice treated with HDM (H), papain (PA), or cockroach (Co) allergens.
 (B and C) Frequencies (B) and numbers (C) of monocytes and moDCs.
 (D) GM-CSF in BAL of mice treated with heat-inactivated (HI), E-64 (E), or AEBSF (A) treated HDM.
 (E–H) B6 mice were left untreated (N) or sensitized. Frequencies of GM-CSF⁺ ncMo (E and F). Frequencies and numbers of monocytes and moDCs (G and H).
 (I–L) Mice were transferred with CD45.1⁺ OT-II.4get cells and treated. Frequencies (I and K) and numbers (J and L) of total and IL-4-GFP⁺ OT-II cells.

Data are representative of at least two independent experiments (mean \pm SD, n = 3–5, one-way ANOVA). *p < 0.05, **p < 0.01, ***p < 0.001, ****p < 0.0001. See Figure S14.

Author Manuscript

Author Manuscript

Author Manuscript

Author Manuscript

KEY RESOURCES TABLE

REAGENT or RESOURCE	SOURCE	IDENTIFIER
Antibodies		
anti-B220 (RA3-6B2)	BD Biosciences	Cat# 552094; RRID:AB_394335
anti-CD3 (17A2)	BD Biosciences	Cat# 561389; RRID:AB_394335
anti-CD4 (GK1.5)	BD Biosciences	Cat# 563050; RRID:AB_2737973
anti-CD11b (M1/70)	BD Biosciences	Cat# 562127; RRID:AB_10893815
anti-CD11c (HL3)	BD Biosciences	Cat# 558079; RRID:AB_647251
anti-CD43 (S7)	BD Biosciences	Cat# 553269; RRID:AB_2255226
anti-CD44 (IM7)	BD Biosciences	Cat# 560780; RRID:AB_1937316
anti-CD45.1 (A20)	BD Biosciences	Cat# 558701; RRID:AB_1645214
anti-CD45.2 (104)	BD Biosciences	Cat# 560695; RRID:AB_1727493
anti-CD62L (MEL-14)	BD Biosciences	Cat# 560514; RRID:AB_10611861
anti-CD90.1 (OX-7)	BD Biosciences	Cat# 561404; RRID:AB_10645378
anti-CD90.2 (53-2.1)	BD Biosciences	Cat# 553007; RRID:AB_398526
anti-CD103 (M290)	BD Biosciences	Cat# 557495; RRID:AB_396732
anti-CD117 (2B8)	BD Biosciences	Cat# 553353; RRID:AB_394804
anti-CCR7 (4B12)	BD Biosciences	Cat# 562675; RRID:AB_2737716
anti-Ly6C (AL-21)	BD Biosciences	Cat# 560596; RRID:AB_1727555
anti-Ly6G (IA8)	BD Biosciences	Cat# 560601; RRID:AB_1727562
anti-NK1.1 (PK136)	BD Biosciences	Cat# 553165; RRID:AB_396674
anti-Siglec-F (E50-2440)	BD Biosciences	Cat# 565183; RRID:AB_2739097
anti-TER-119 (TER-119)	BD Biosciences	Cat# 553673; RRID:AB_394986
anti-CD64 (X54-5/7.1)	Biolegend	Cat# 139306; RRID:AB_11219391
anti-CCR2 (SA203G11)	Biolegend	Cat# 150605; RRID:AB_2571913
anti-CX3CR1 (SA011F11)	Biolegend	Cat# 149005; RRID:AB_2564314
anti-Fc epsilon RI alpha (MAR-1)	Biolegend	Cat# 134306; RRID:AB_1626108
anti-MHC class II (M5/114.15.2)	Biolegend	Cat# 107620; RRID:AB_493527
and anti-XCR1 (ZET)	Biolegend	Cat# 148212; RRID:AB_2564367
anti-CD49b (DX5)	eBioscience	Cat# 17-5971-82; RRID:AB_469485
anti-CD115 (AFS98)	eBioscience	Cat# 13-1152-85; RRID:AB_466565
anti-CD127 (A7R34)	eBioscience	Cat# 25-1271-82; RRID:AB_469649
anti-mertK (DS5MMER)	eBioscience	Cat# 17-5751-82; RRID:AB_2716943
anti-IL-13 (13A)	eBiosciences	Cat# 12-7133-41; RRID:AB_10852712
anti-IL-5 (TRFK5)	BioLegend	Cat# 504311; RRID:AB_2563161
anti-IFN γ (XMG1.2)	BD Biosciences	Cat# 557649; RRID:AB_396766
anti-IL-2 (JES6 5H4)	BD Biosciences	Cat# 562041; RRID:AB_398555
anti-IL-12 (C15.6)	BD-Biosciences	Cat# 554479; RRID:AB_395420
anti-TNF α (MP6-XT22)	BD-Biosciences	Cat# 554418; RRID:AB_395379
anti-IL-1 β (NJTEN3)	eBioscience	Cat# 17-7114-80; RRID:AB_10670739
anti-GM-CSF (MP1-22 $\times 10^9$)	eBioscience	Cat# 12-7331-82; RRID:AB_466205
anti-T-bet (4B10)	biolegend	Cat# 644814; RRID:AB_10901173

REAGENT or RESOURCE	SOURCE	IDENTIFIER
anti- CD16/32 (2.4G2)	BioXCell	Cat# CUS-HB-197; RRID:AB_2687830
anti-CCL2 (MCP-1)	BioXCell	Cat# BE0185; RRID:AB_10950302
anti-GM-CSF (MP1-22 × 10 ⁹)	BioXCell	Cat# BE0259; RRID:AB_2687738
anti-Ly6G (1A8)	BioXCell	Cat# BP0075-1; RRID:AB_1107721
Anti-IgE	Southern Biotech	Cat# BP0075-1; RRID:AB_2794604
Chemicals, peptides, and recombinant proteins		
EndoFit ovalbumin	InvivoGen	Cat# NC1005858
Diphtheria toxin	Sigma-Aldrich	Cat# D0564-1MG
PMA	Sigma-Aldrich	Cat# P8139-1MG
Calcimycin	Life Technologies	Cat# A1493
Papain from papaya latex	Sigma-Aldrich	Cat# P5306-25MG
Recombinant mouse GM-CSF	PeptoTech	Cat# 315-03
Clodronate liposomes	Encapsula NanoSciences	Cat# CLD-8909
Cysteine protease inhibitor E-64	Sigma-Aldrich	Cat# E3132
Serine protease inhibitor AEBSF	Sigma-Aldrich	Cat# A8456
Chitinase	Millipore Sigma	Cat# SAE0158
Beta-(1->3)-D-Glucanase	Sigma-Aldrich	Cat# 67,138
Collagenase A	Sigma-Aldrich	Cat# C7657
Deoxyribonuclease I from bovine pancreas	Sigma-Aldrich	Cat# D4527
Critical commercial assays		
Transcription factor staining buffer set	eBioscience	Cat# 00-5523-00
BD Cytofix/Cytoperm Fixation/Permeabilization Solution Kit with GolgiPlug™	BD Biosciences	Cat# 555028
Anti-L3T4 (CD4) Microbeads, mouse	Miltenyi Biotec	Cat# 130-049-201; RRID:AB_2722753
CD11c MicroBeads UltraPure, mouse	Miltenyi Biotec	Cat# 130-108-338
CellTrace Violet Cell Proliferation Kit	ThermoFisher	Cat# C34557
AF647 labeling kit	Invitrogen	Cat# A20173
GM-CSF Mouse Uncoated ELISA Kit with Plates	Invitrogen	Cat# 50-112-8722
Mouse TNF-alpha Quantikine ELISA Kit	R&D Systems	Cat# MTA00B
RNeasy Plus Micro Kit	QIAGEN	Cat# 74034
Deposited data		
BM monocytes, stimulated with PBS (Ctrl, labeled as AH1,2,3) or GM-CSF (Ctrl, labeled as AGM1,2,3) for 3h	This paper	GEO: GSE186449
Experimental models: Organisms/strains		
House dust mite (<i>Dermatophagoides pteronyssinus</i> and <i>Dermatophagoides farinae</i>) extract	Greer laboratories	N/A
German Cockroach (<i>Blattella germanica</i>) extract	Greer laboratories	N/A
Lipopolysaccharide from <i>Escherichia coli</i> 0111:B4	Sigma-Aldrich	Cat# L2630
Mouse: C57BL/6J (B6)	The Jackson Laboratory	Stock No: 000664
Mouse: B6.SJL- <i>Ptpr</i> ^{ca} <i>Pepc</i> ^{fl} /BoyJ (CD45.1 ⁺ B6 congenic)	The Jackson Laboratory	Stock No: 002014
Mouse: C57BL/6-Tg(TeraTerb)425Cbn/J (OT-II)	The Jackson Laboratory	Stock No: 004194
Mouse: B6.129-Il4 ^{tm1Lky} /J (B6.4get IL-4 reporter mice)	Laboratory of Dr. M. Mohrs (Trudeau Institute)	N/A

REAGENT or RESOURCE	SOURCE	IDENTIFIER
Mouse: C.129-II4tm1Lky/J (BALB/c.4get IL-4 reporter mice)	The Jackson Laboratory	Stock No: 004190
Mouse: B6(Cg)-Tlr4tm1.2Karp/J (<i>Tlr4</i> ^{-/-})	The Jackson Laboratory	Stock No: 029015
Mouse: B6.129S1-II12atm1Jm/J (<i>Il12a</i> ^{-/-})	The Jackson Laboratory	Stock No: 002692
Mouse: C57Bl/6J-Tg(Itgax-cre,-EGFP) 4097Ach/J (<i>Itgax-cre,-EGFP</i>)	The Jackson Laboratory	Stock No: 007567
Mouse: B6.129S4-Ccr2tm1Hfc/J (<i>Ccr2</i> ^{-/-})	The Jackson Laboratory	Stock No: 004999
Mouse: BALB/cJ (BALB/c)	The Jackson Laboratory	Stock No: 000651
Mouse: C.Cg-Tg(DO11.10)10Dlo/J (D011.10)	The Jackson Laboratory	Stock No: 003303
Mouse: CBy.PL(B6)-Thy1a/ScrJ (BALB/c Thy1.1 ⁺)	The Jackson Laboratory	Stock No: 005443
Mouse: B6.129S-Csf2tm1Mlg/J (<i>Csf2</i> ^{-/-})	The Jackson Laboratory	Stock No: 026812
Mouse: B6; 129S-Tnfrtm1Gkl/J (<i>TNFA</i> ^{-/-})	The Jackson Laboratory	Stock No: 005540
Mouse: B6.Cg-KitW-sh/HNhrJaeBsmJ (cKitw-sh)	The Jackson Laboratory	Stock No: 030764
Prism V9	GraphPad	https://www.graphpad.com/
FlowJo V9.9.6	TreeStar	https://www.flowjo.com
javaGSEA V7.0	Broad Institute	http://www.gsea-msigdb.org/gsea/index.jsp
R2021b	MATLAB	https://www.mathworks.com/products/matlab/whatsnew.html
R package edgeR	Bioconductor	https://bioconductor.org/packages/release/bioc/html/edgeR.html